Milena Huhnen-Venedey

Spectroscopy of Stars

Development of a new Laboratory Course

Diplomarbeit in Physik

Angefertigt im Argelander-Institut für Astronomie.
Vorgelegt der Mathematisch-Naturwissenschaftlichen Fakultät
der Rheinischen Friedrich-Wilhelms-Universität Bonn.

September 2011

Referent	Prof. Dr. Norbert Langer
Korreferent	Prof. Dr. Robert Izzard

Erklärung

Hiermit versichere ich, dass ich diese Arbeit selbständig verfasst und keine anderen als die angegebenen Quellen und Hilfsmittel benutzt sowie Zitate kenntlich gemacht habe.

Bonn, im September 2011

Contents

Chapter 1

Introduction

The thesis describes the development of a new laboratory course in optical astronomical spectroscopy for third year Bachelor students at the University of Bonn. It includes all manuals needed as well as detailed explanations of the instrumental set-up used for the laboratory course. The course was already proven in a test run in early summer 2011 and was successfully completed by three groups of students, who received full credit points for it. The test run showed that the assignment of tasks was appropriate for the given time frame. The next student groups will come in October 2011.

The name of the laboratory course, "Spectroscopy of Stars", indicates that the students will take spectra of astronomical objects. Spectroscopy is a fundamental and important part of astronomical observations. It started in the early nineteenth century, when *Joseph von Fraunhofer* discovered the spectral lines in the solar spectrum, which are now known as Fraunhofer lines. Soon afterwards he observed dark lines in the spectra of other stars, but could not immediately explain them. It was not until 1859 that *Gustav Kirchhoff* published the fundamental (Kirchhoff's) laws which led to a new understanding of spectroscopy. Stellar spectroscopy and the understanding of the nature of atoms and hence of the physical processes underlying the production of spectra developed parallel.

With stellar spectroscopy it can be derived a variety of physical phenomena such as temperature and chemical composition of astronomical objects. Intrinsic rotation of stars is one of the dominant line broadening mechanism in stellar spectroscopy. With the observation of the 21 cm line of neutral hydrogen it is even possible to derive the rotation of the Milky Way. Spectral lines are also used to measure outflows from stars, and in case the resolution of the spectrograph is high enough even magnetic fields can be measured by finding spectral lines corresponding to the Zeeman effect. The mass of binary star systems can be determined and the oscillation of stars is also measurable.

The possibilities for tasks used in a laboratory course are manifold but it was decided to put the center of attention on the Doppler effect because it had to be kept in mind what would actually be possible to measure with the given set-up and what would be appropriate for the students in the given time frame. Motions of different objects (e.g. two stars orbiting each other, rotation of a star, stellar winds) will lead to Doppler shifted or Doppler broadened spectral lines. The second chapter of this thesis contains the determination of the resolution of the spectrograph to estimate what is possible to measure with the set-up. Based on the resolution of the spectrograph (and by keeping in mind that it was important to keep the content demanding but not overstraining), it was decided that the students will observe:

- a binary star system to determine its total mass,
- a fast rotating star to determine its rotational velocity,
- the strong emission lines of Wolf-Rayet stars to determine the wind velocity.

By considering these phenomena, the students will learn how to handle a telescope, a spectrograph and a CCD camera, with the technical background such as functionality of a CCD including data reduction, theory of diffraction gratings and coordinate systems. Furthermore, it will deepen their knowledge of atomic physics, spectroscopy, line broadening mechanisms and the Doppler effect. During the laboratory course students will, among other things, develop an understanding of the geometry of binary stars, Kepler's laws, and how these relate to the Doppler effect. Data are reduced and analyzed with a modern computer software (IRAF - Image Reduction and Analysis Facility) and a numerical simulation is required to accomplish these tasks. The students must carefully plan their observations to obtain useful data, thus, in addition to the reduction process, they learn how to work and write scientifically. The laboratory course challenges the students and makes a valuable contribution to the Bachelor astrophysics course.

This thesis is structured in the following order. In Chapter 2 the experimental setup is explained, including detailed examinations of the individual components. Furthermore in Chapter 3 and 4, the phenomena to be analyzed are presented as well as the observing and data analysis methods. Finally, the appendix includes the test record and useful information that will be handed out to the students for the completion of the laboratory course.

Chapter 2

The Instruments

For the development of the new laboratory course, a spectrograph and CCD camera were purchased. The DADOS spectrograph was designed at the Max-Planck-Institute for extraterrestrial physics in Garching, Germany. It was developed a sophisticated instrument perfectly suited for use in schools or Universities. Baader Planetarium introduced a prototype of the spectrograph before it was manufactured, and because of ratings in different spectroscopy forums[1], changes were made in its concept so the final product is respectable. The camera is an SBIG ST 402 ME from Santa Barbara Instrument Group (USA). The camera has a CCD chip (KAF 0402 ME) which has, compared to other cameras in the same price range, a good quality and is the camera recommended by the producer of the spectrograph to be used with the DADOS.

2.1 The Spectrograph

In the following sections the spectrograph will be described in more detail. First its construction is explained, then its resolution determined. Finally a measurement to determine the best focus for the spectrograph with the ST 402 ME camera was carried out. To wavelength-calibrate the spectra a calibration lamp is needed; the lamp is described in Section 2.1.4.

2.1.1 Construction

Figure 2.1 shows a schematic depiction of the DADOS spectrograph. Light enters the aperture and illuminates three slits; the slits have sizes of 25 µm, 35 µm and 50 µm. Through the slit viewer it can be seen if the starlight is accurately placed on the desired slit. The angle of incidence (on the diffraction grating) determines the wavelength range displayed on the chip and is set by a micrometer screw. The light is deflected by the diffraction grating[2] and then focused on the camera, or eyepiece. Figure 2.2 shows an image of the spectrograph, to change the focus, the focuser marked with the circle has to be adjusted. The figure also shows the camera, the calibration lamp and the mount which gives the whole set-up more stability.

2.1.2 Resolution of the Spectrograph

The spectral resolution R, is defined as

[1] For example: `http://spektroskopie.fg-vds.de/` accessed on September 5., 2011.
[2] It can be chosen between a 200- and a 900-line grating (per mm).

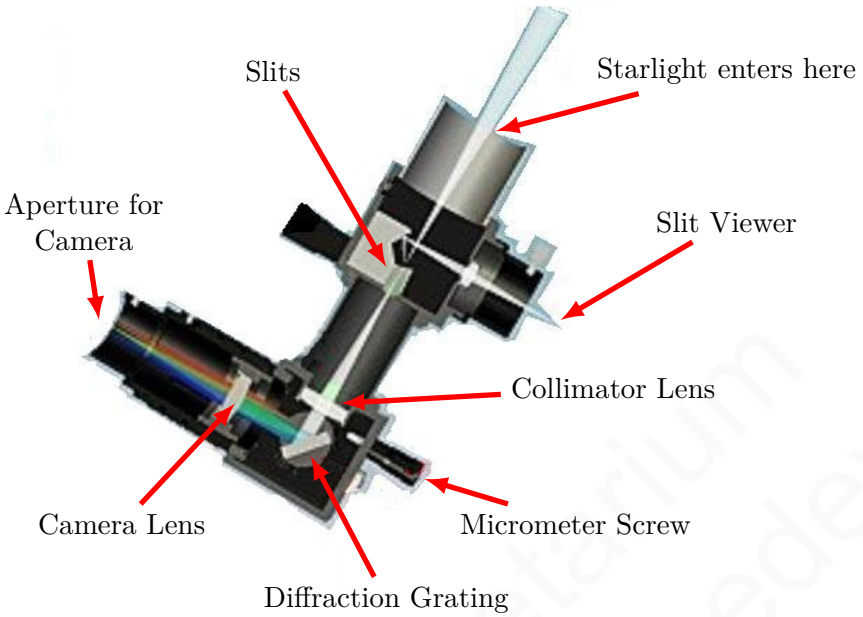

Figure 2.1: Schematic depiction of the DADOS spectrograph. For further explanation see Section 2.1.1 (from `http://www.baader-planetarium.de/dados/dados.htm`, accessed on August 29., 2011).

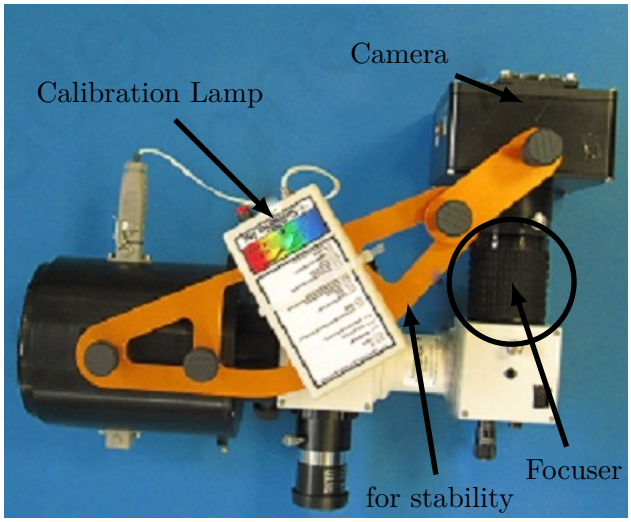

Figure 2.2: Picture of the complete set-up with DADOS spectrograph, camera and calibration lamp. The yellow mount gives the set-up more stability.

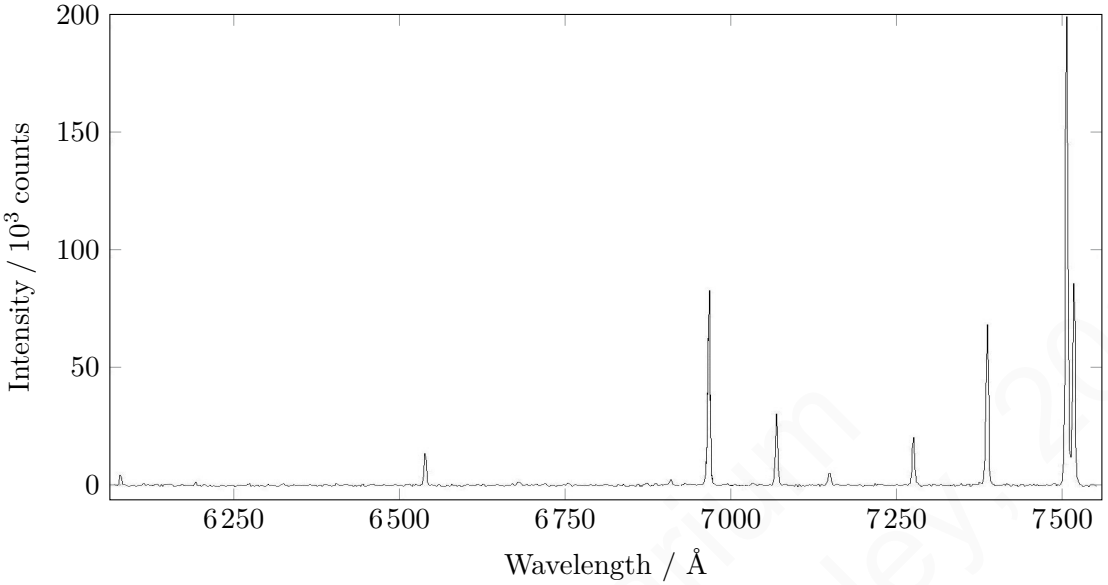

Figure 2.3: A spectrum of the calibration lamp which was wavelength calibrated with IRAF. This gives one example of the spectra used to determine the resolution of the DADOS spectrograph. This spectrum was taken with the 200-line grating at first order.

$$R = \frac{\lambda}{\Delta\lambda} = mN \quad , \tag{2.1}$$

where λ is the observed wavelength, $\Delta\lambda$ is the smallest wavelength difference that can be resolved, m is the number of illuminated grating slits and N the order at which the resolution is determined.

The spectral resolution as a function of wavelength was determined for both gratings by taking spectra of the calibration lamp. The spectral lines were identified and the widths measured using IRAF by fitting Gaussian functions to the spectral lines. Appendix B describes the extraction of the spectra and wavelength calibration. Tables 2.1 and 2.2 contain the results, and, in Fig. 2.3, the spectrum of an arbitrary wavelength range of the calibration lamp is shown as an example. The resolution of the DADOS spectrograph, as stated by the manufacturer, is shown in Fig. 2.4. As expected is the resolution of the 900-line grating more than 4 times better than that of the 200-line grating. Only the 900-line grating was used for observation to benefit from the better resolution.

2.1.3 Measurement to find the best focus for the spectrograph

To find the best focus setting for the spectrograph the full-width-half-maximum (FWHM) of a spectral line (of the calibration lamp, see Section 2.1.4) was measured as a function of the spectrograph focus. The calculation of the full-width-half-maximum was done

λ / Å	**FWHM** / Å	**FWHM** / km s^{-1}	**R**
8264	2.255	82	3665
8115	2.261	84	3589
7948	2.289	86	3472
7723	2.323	90	3325
7635	2.285	90	3341
7504	2.237	89	3354
7384	2.195	89	3364
7272	2.223	92	3271
7067	2.067	88	3419
6965	2.085	90	3341
5790	1.736	90	3335
5769	1.723	90	3348
5460	1.769	97	3087
4358	1.666	115	2616
4046	1.960	145	2064
3650	3.268	268	1117

Table 2.1: Resolution R of the 900-line grating of the DADOS spectrograph. The resolution was determined using spectra of the calibration lamp. The widths of the spectral lines were determined using the Gaussian fit utility of IRAF. The displayed full-width-half-maxima (FWHM) represent the widths of the instrumental line profile, which is dependent on wavelength. The last entry (3650 Å) is blended with other lines so the width is broader than for the other entries. Converted with the Doppler Equation (3.1), the linewidths can also be given in km s^{-1}.

λ / Å	**FWHM** / Å	**FWHM** / km s^{-1}	**R**
8264	12.7	461	650
7723	11.6	448	669
7635	9.8	386	776
6965	9.4	406	739
5460	7.7	421	713
4358	7.7	531	565

Table 2.2: Resolution R of the 200-line grating of the DADOS spectrograph. The resolution was determined using the calibration lamp spectra. The widths of the spectral lines were determined via Gaussian fits (done by IRAF). The displayed full-width-half-maxima represent the widths of the instrumental line profile which is dependent on wavelength. Converted with the Doppler Equation (3.1), the linewidths can also be given in km s^{-1}.

Resolving power λ / Δ λ on camera objective axis and 25 µm slit

Grating of 200 lines/mm

Theoretical	Measured	λ (nm)
396	542	@ 416
606	647	@ 616
668	723	@ 697

Grating of 900 lines/mm

Theoretical	Measured	λ (nm)
2038	2000	@ 371
3910	3000	@ 561
5376	5000	@ 800

Figure 2.4: Resolution of the DADOS spectrograph as stated by the manufacturer, *Baader Planetarium*. As one can see, the values determined during the preparation of this lab course, are consistent with these provided by the manufacturer.

with IRAF, using a Gaussian fit. Because of the lack of a physical scale, the scale talked about below is that of a strip of paper glued to the spectrograph with a scale in scale marks (scale divisions). Scale divisions specifiy divisions of equidistant separations on a scale. The measurement was done to *approximately* determine the optimal focus. After completion of the measurement, the best positions for the two gratings were marked on the spectrograph. It was decided not to calculate the error on the results because this measurement was intended to get an overview and to mark *approximately* the setting of the optimal focusing position and not to determine the exact position. A vernier adjustment was done at the beginning of each night. The data were fitted with a second order polynomial. The fitting formula was

$$f(x) = a_1(x + a_2)^2 + a_3 \quad ,$$

where a_1, a_2 and a_3 are the fitting parameters. a_1 gives the dilation of the parabola, a_2 the shift on the x axis and a_3 the offset. The angular point would have the coordinates $(-a_2/a_3)$.
Figures 2.5, 2.6 and 2.7 show the fits for the three different slits. The minimum of the full-width-half-maximum for all three slits occurs at 25 µm.

Table 2.3 shows the fit parameters and the RMS[3] residuals. The best adjustment for the focus for the 900-line grating is approximately 18.4 scale divisions. The focus changes slightly for the 200-line grating.

[3]Root Mean Square.

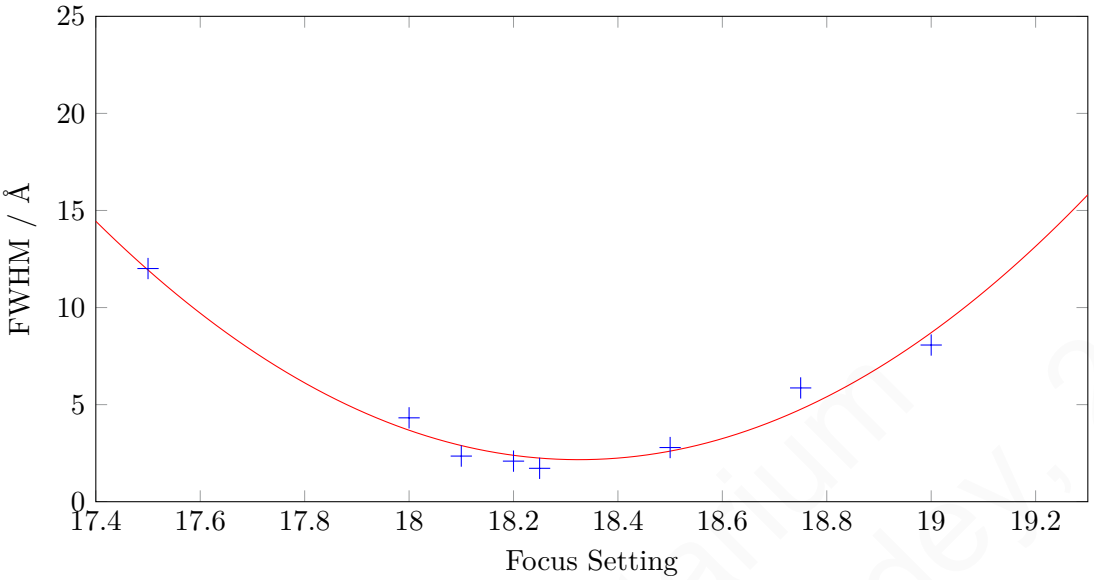

Figure 2.5: The full-width-half-maximum of a spectral line (7067 Å) of the calibration lamp (see Section 2.1.4) vs. adjustment of the focus setting. The slit width was selected to be 50 µm and the 900-line grating was used.

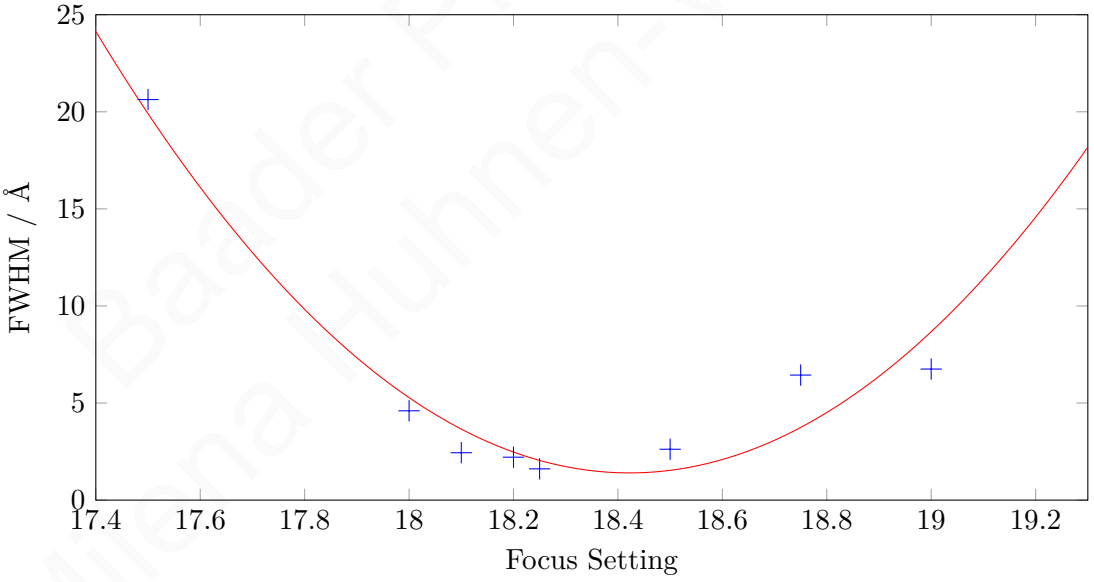

Figure 2.6: The full-width-half-maximum of a spectral line (7067 Å) of the calibration lamp (see Section 2.1.4) vs. adjustment of the focus setting. The slit width was selected to be 25 µm and the 900-line grating was used.

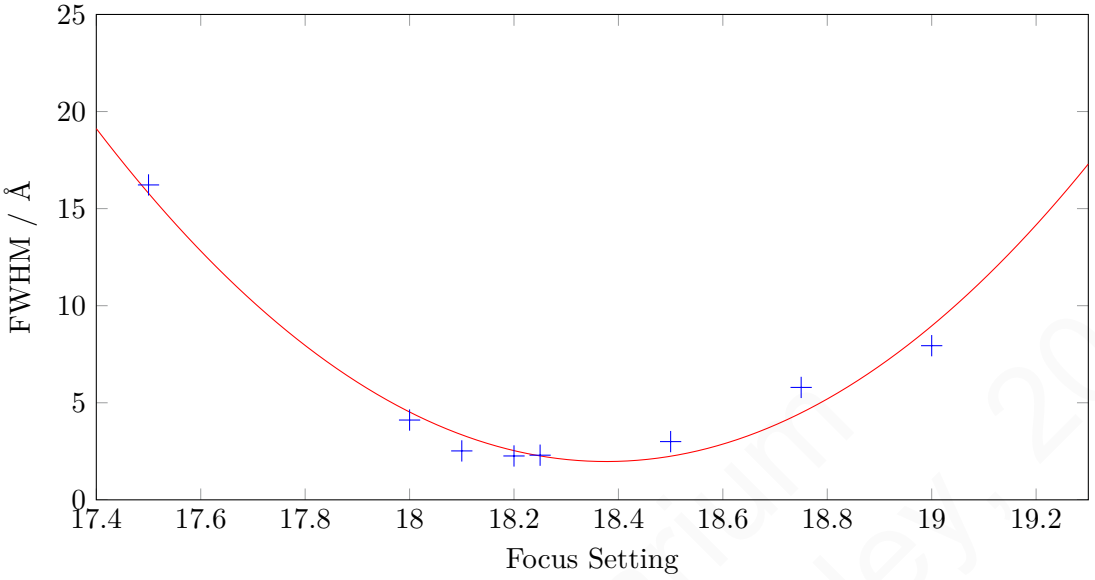

Figure 2.7: The full-width-half-maximum of a spectral line (7067 Å) of the calibration lamp (see Section 2.1.4) vs. adjustment of the focus setting. The slit width was selected to be 35 µm and the 900-line grating was used.

slit size	a_2 **/ scale divisions**	a_3 / Å	**RMS**
50 µm	18.38	1.97	0.943
25 µm	18.42	1.40	1.725
35 µm	18.33	2.17	0.738

Table 2.3: Fit parameters for the three slits obtained via a second order fit to the data. These parameters can be used to determine the optimal focus setting for the spectrograph.

2.1.4 The calibration lamp

The SL2 calibration lamp of *StellarNet Inc* was chosen for calibration of the stellar spectra. It provides mercury and argon gas emission lines with wavelengths from 2356.5 Å to 10139.8 Å. Figure 2.8 shows the complete spectrum of the calibration lamp taken at, and with the equipment of, the IAP[4]. Figure 2.9 gives an example of the spectrum of the calibration lamp taken with the set-up of the laboratory course. It should be noted that the final observations are obtained only with the 900-line grating at first order. The spectrograph has a micrometer screw to tilt the grating such that different wavelengths of the spectrum are imaged on the camera's CCD chip. Figure 2.10 (900-line grating) and Fig. 2.11 (200-line grating) show graphically how the mean wavelength imaged on the camera chip depends on the adjustment of the micrometer screw. The horizontal

[4]Institut für Angewandte Physik der Universität Bonn.

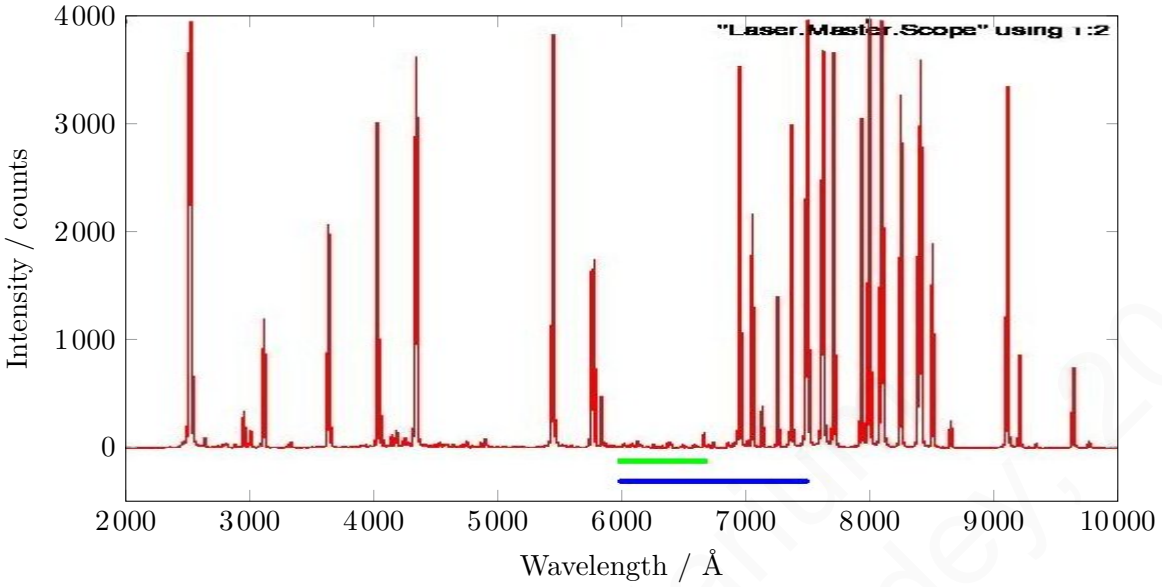

Figure 2.8: Complete spectrum of the mercury/argon calibration lamp. The green (shorter) dash indicates the wavelength range displayed on the CCD with the 900-line grating (approximately 730 Å); the blue (longer) dash indicates the wavelength range displayed when using the 200-line grating (approximately 1400 Å).

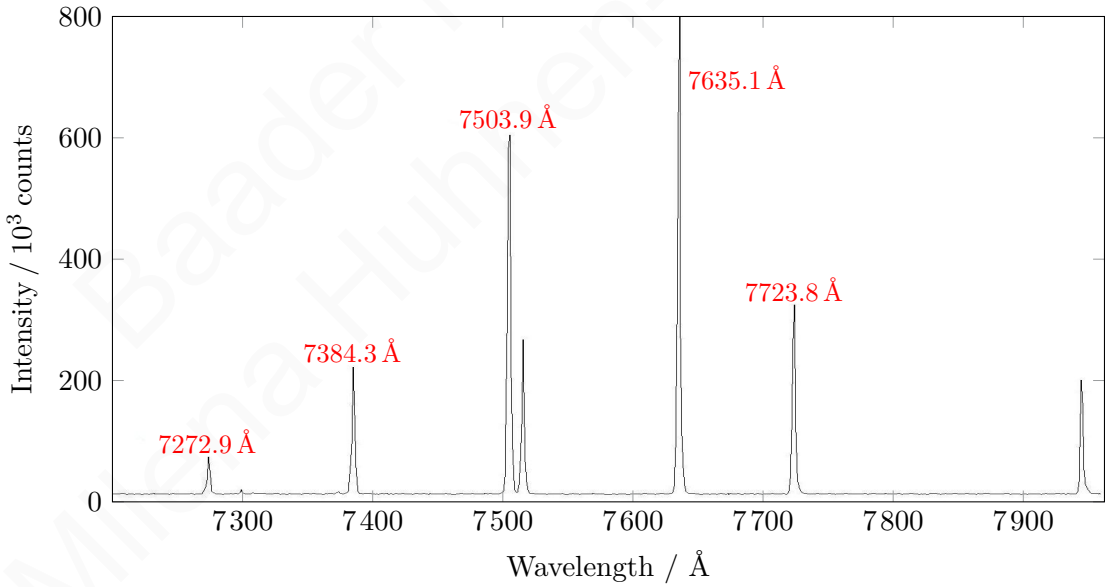

Figure 2.9: Ordinary Spectrum of the calibration lamp taken at first order with the 900-line grating. This is just a part of the spectrum (approximately 700 Å).

micrometer screw / µm	**wavelength range** / Å	$\Delta\lambda$ / Å	$\lambda_{\mathbf{mean}}$ / Å
0	7200 - 7950	750	7575
55	6500 - 7250	750	6875
110	5785 - 6550	765	6165
165	5170 - 5880	710	5525
220	3910 - 4590	680	4250

(a) 900-line grating

micrometer screw / µm	**wavelength range** / Å	$\Delta\lambda$ / Å	$\lambda_{\mathbf{mean}}$ / Å
0	9100 - 7650	1450	8375
20	8500 - 7000	1500	7750
50	7500 - 6100	1400	6800
80	6600 - 5250	1350	5925
110	5650 - 4250	1400	4950

(b) 200-line grating

Table 2.4: This Table lists the wavelength ranges imaged on the chip as a function of the values of the micrometer screw for the two different gratings. $\Delta\lambda$ is the wavelength range projected on the chip for the given λ_{mean}. The mean displayed wavelength λ_{mean} is also given.

bars indicate the wavelength range for each grating, which is approximately 730 Å for the 900-line grating and approximately 1400 Å for the 200-line grating. Tables 2.4a and 2.4b list the associated data. To calculate the setting of the micrometer screw, one can use the following equation for a given center-wavelength λ:

$$f(\lambda) = -0.083\lambda + 623.78 \quad ,$$

and

$$f(\lambda) = -0.032\lambda + 270 \quad ,$$

for the 900- and 200-line gratings, respectively.

2.2 The Camera

The camera is an SBIG ST 402 ME from *Santa Barbara Instrument Group Inc.*. Figure 2.12 shows the parameters of the camera as provided by the manufacturer. Figure 2.13 shows the quantum efficiency of the camera's chip: a Kodak KAF 0402 ME CCD. The camera is compact, affordable and easy to use, which is important for students without much laboratory experience. The pixel scale is 0.9 Å/pixel (900-line grating). The camera is operated using the program CCD SOFT.[5]

[5] The CCD SOFT manual can be found on `http://www.bisque.com/help/ccdsoft\%20info/ccdsoft_version_5_user_s_manual.htm`, accessed on September 5., 2011.

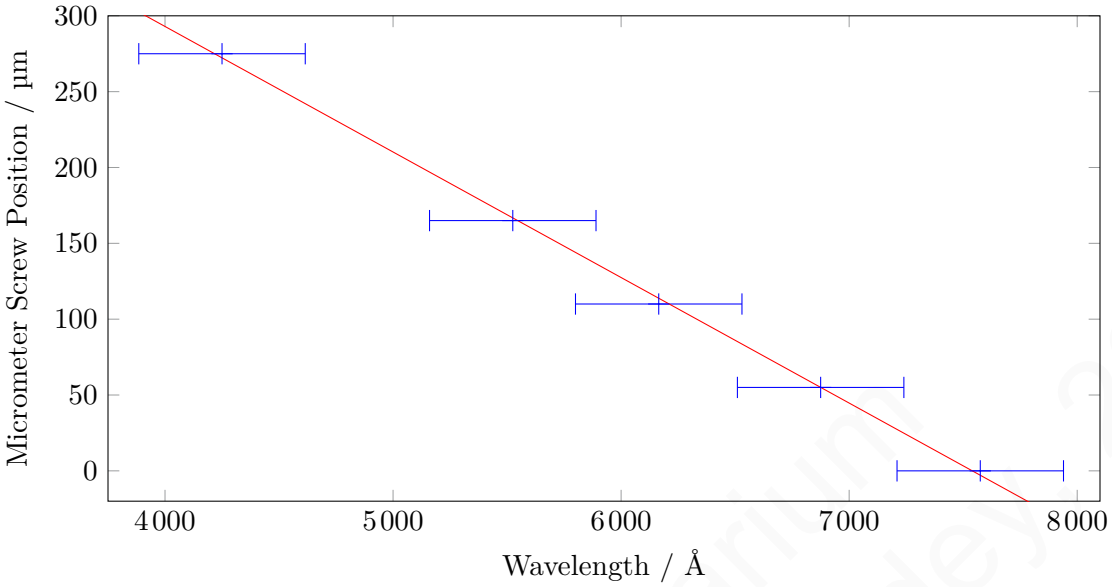

Figure 2.10: Center wavelength displayed on the CCD chip as a function of the adjustment of the micrometer screw for the 900-line grating. The horizontal bars indicate the total wavelength range displayed on the chip, which is approximately 730 Å for the 900-line grating.

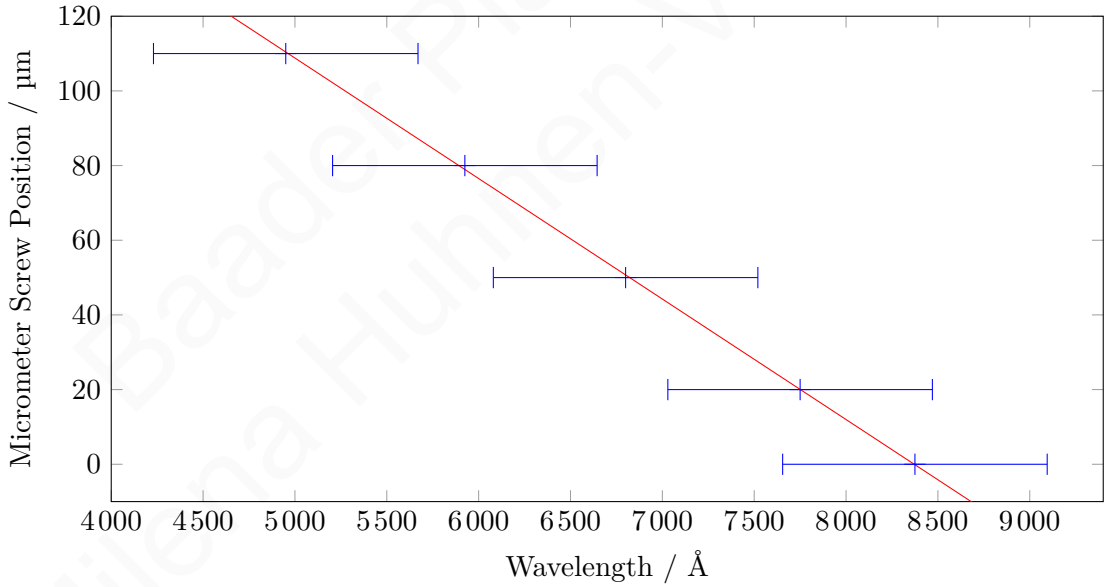

Figure 2.11: Center wavelength imaged on the CCD chip as a function of the adjustment of the micrometer screw for the 200-line grating. The horizontal bars indicate the total wavelength range imaged on the chip, which is approximately 1400 Å for the 200-line grating.

CCD	
CCD	Kodak KAF-0402ME
Pixel Array	765 x 510 pixels
CCD Size	6.9 x 4.3 mm
Total Pixels	390,000
Pixel Size	9 x 9 microns
Full Well Capacity	~100,000 e-
Dark Current	1e¯/pixel/sec at 0° C
Antiblooming	Optional

Readout Specifications	
Shutter	Electromechanical
Exposure	0.09 to 3600 seconds, 10ms resolution
Correlated Double Sampling	Yes
A/D Converter	16 bits
A/D Gain	1.5e- unbinned 2.0e- binned 2x2, 3x3 (1.0e- and 1.4e- for ABG CCD)
Read Noise	13.8e¯ RMS Typical
Binning Modes	1 x 1, 2 x 2, 3 x 3
Pixel Digitization Rate	Up to 800,000 pixels per second with USB 2.0
Full Frame Download	<1 second

System Specifications	
Cooling - Enhanced	Single Stage Thermoelectric, Active Fan, -30 C from Ambient Typical
Cooling - Standard	Single Stage Thermoelectric, Active Fan, -20 C from Ambient Typical
Temperature Regulation	±0.1°C
Power	12VDC Power supply included
Computer Interface	USB 2.0 (USB 1.1 compatible)
Computer Compatibility	Windows 98/2000/Me/XP Mac OS-X

Physical Dimensions	
Optical Head	5 x 4 x 2.5 inches (including fan)
CPU	All electronics integrated into Optical Head, No CPU
Mounting	T-Thread, 1.25" nosepieces included
Weight	Approx. 20 oz. (0.6kg)
Backfocus (C-mount compatible)	0.69 inches

Figure 2.12: Parameters of SBIG ST 402 ME given by the manufacturer. From `http://www.sbig.com/ST-402ME-C1.html`, accessed on September 13., 2011.

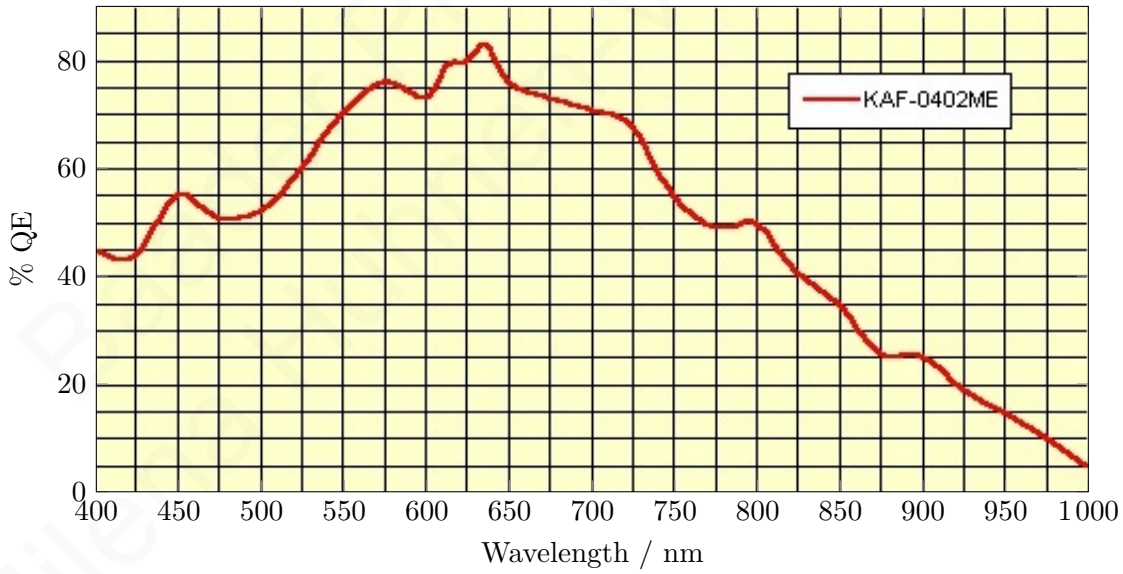

Figure 2.13: Quantum Efficiency of the KAF 0402 ME chip. The best quantum efficiency lies around 6500 Å, this wavelength corresponds approximately to the wavelength of the Hα line of hydrogen (6562.8 Å). From `http://www.sbig.de/bilder/qe_st402me.gif`, accessed on September 13., 2011.

2.2.1 Determining gain and readnoise

The gain is the conversion factor with which the number of counts is converted into the number of electrons. The readnoise is the noise per pixel (in counts) generated by the read-out procedure of the CCD chip. Gain K and readnoise N_R of the camera were determined using the method described in Howell (2006), page 53. The gain K is given by

$$K = \frac{(F_1 - F_2) - (B_1 - B_2)}{\sigma^2_{F_1-F_2} - \sigma^2_{B_1-B_2}} \quad ,$$

where $F_{1,2}$ and $B_{1,2}$ are mean intensity values of two flat fields and bias frames[6], respectively. $\sigma_{F_1-F_2}$ and $\sigma_{B_1-B_2}$ are the standard deviations of the intensity of a difference image of F_1 and F_2 and of B_1 and B_2, respectively.

The readnoise N_R is given by

$$N_R = \frac{K \cdot \sigma_{B_1-B_2}}{\sqrt{2}} \quad .$$

The results for the adapted set-up were:

- Gain $K = 1.5\,\text{electrons/count}$
- Readnoise $M = 17.8\,\text{electrons/pixel}$

Figure 2.12 gives, amongst other things, the gain and readnoise determined by the manufacturer. The values given by the manufacturer and the ones determined here are compatible. Error analysis for the (camera's) orientation values was neglected since their main purpose was to test the parameters given by the manufacturer.

2.2.2 Determination of the signal-to-noise ratio

Any experimental signal is biased by noise. Figure 2.14 shows schematically the several individual contributions to a measured signal (e.g. a spectral line). The level of the signal is a combination of the signal, the dark level (due to dark current), the bias level (due to the bias offset[7]) and the sky brightness level (due to stray light from the sky surrounding the star). To get the pure signal (still overlaid with the Poisson noise) one has to subtract these three levels. The effect of the Poisson noise is visible in Fig. 2.14 as fluctuations about the true signal: The higher the signal, the higher the Poisson noise ($\propto \sqrt{N}$, where N is the number of counts).

[6] Flat field frames and bias frames are calibration frames used in data reduction processes. A detailed explanation of how and why to reduce the data is given in Howell (2006).

[7] See Howell (2006) for details.

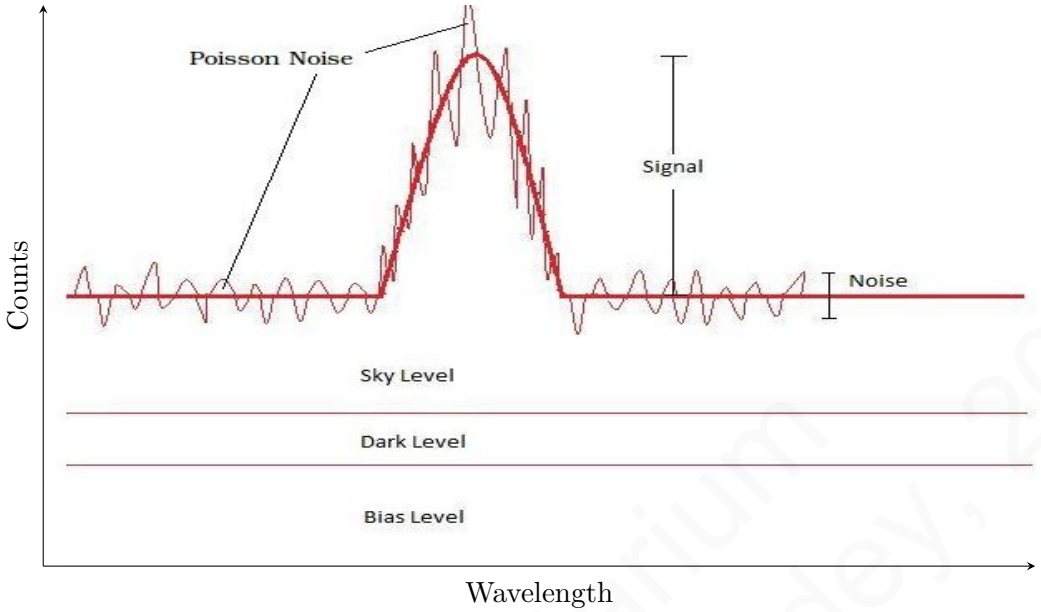

Figure 2.14: The contributions of various forms of background noise to a measured signal. The signal is a combination of true signal, dark level, bias level and sky level. The Poisson noise is demonstrated schematically, the higher the signal, the higher is the Poisson noise ($\propto \sqrt{N}$, where N is the number of counts).

Figure 2.15 shows the dependency of the dark current emitted by the KAF 0402 ME (in counts) on exposure time t at a temperature of $-5\,°\mathrm{C}$. This measurement was performed to get an overview of the produced dark current. It was decided not to calculate the uncertainties because the exact amount of dark current was not a desired quantity. It was intended to test the parameters given by the manufacturer. The data are accurately described by the following linear function

$$f(t) = 1.95t + 980.16 \quad . \tag{2.2}$$

The intersection point with the y axis gives the bias level (980.16 counts). To get an overview about the necessary exposure time for a star as a function of its magnitude and the desired signal-to-noise ratio, spectra of stars of different magnitudes were taken and their signal-to-noise ratios determined at wavelengths around 6600 Å. Note, that the signal-to-noise ratio depends also on the focus of telescope and spectrograph and on the weather (seeing). During the preparation of the laboratory course it proved necessary to obtain at least a signal-to-noise ratio of 35 in order to work with the spectra.
The signal-to-noise ratio was calculated with the so-called "CCD Equation" from Howell (2006):

$$\frac{S}{N} = \frac{N_*}{\sqrt{N_* + n_{\mathrm{pix}}(N_S + N_D + {N_R}^2)}} \quad . \tag{2.3}$$

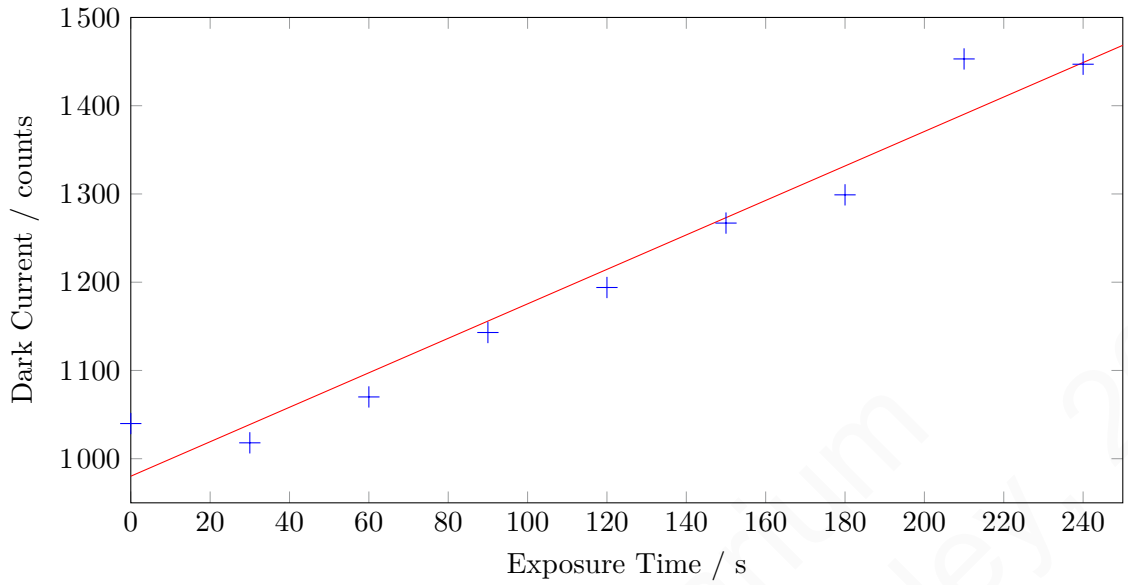

Figure 2.15: Dependency of dark current on the exposure time (as expected the relation is described by a linear function). With this relation one can *estimate* the dark current level for a given time span at a temperature of −5 °C. This measurement was performed to get an overview of the produced dark current. It was consciously decided not to calculate the uncertainties.

In Equation 2.3 is

- S the Signal,
- N the Noise,
- N_* the Number of electrons produced by the star,
- n_{pix} the number of pixels,
- N_S the Number of electrons produced by sky and background,
- N_D the Number of electrons produced by dark current and
- N_R is the readnoise.

Table 2.5 shows stars of different magnitudes and exposure times and the calculated signal-to-noise ratios.

star name	magnitude of star	T_{exp}/ s	S/N ratio
Vega	0.03	5	20
		15	22
		30	39
		60	37
		120	43
Regulus	1.36	10	13
		30	29
		60	32
SAO 61391	3.92	5	7
		10	7
		30	9
		60	16
		120	17
		300	39
AO Cassiopeiae	6.102	1200	28

Table 2.5: Signal-to-noise ratios determined with the IRAF task *imexam*. The individual signal-to-noise ratio was determined in a narrow region in the continuum of the stellar spectrum in the original, two dimensional image before extraction of the spectrum. Note, that the signal-to-noise ratio depends also on the focus of telescope and spectrograph and on the weather (seeing). For example, it is shown here that after an exposure time of twenty minutes, the signal-to-noise ratio of AO Cassiopeia was still lower than 35. AO Cassiopeia rose late in that night and dawn already started. Nevertheless it is possible to obtain useful data of AO Cassiopeia with exposure times of 600 s. The detailed method how to determine the signal-to-noise ratio is described in Appendix B.9. The magnitudes of the stars were taken from `http://simbad.u-strasbg.fr/simbad/`, accessed on August 29., 2011.

2.3 The Telescope

The telescope used to collect data for this diploma thesis is a Cassegrain type telescope with a 50 cm primary mirror and a focal length of 450 cm. The f-ratio is f/9 for the Cassegrain focus and f/3 for the primary focus. The telescope was mounted on the roof of the Argelander Institut für Astronomie in summer 2009 and is electronically controlled using the program AUTOSLEW, written by *Philipp Keller, AstroOptik*.

2.3.1 The AIfA 50 cm-Telescope

Figure 2.16 shows the telescope set-up with its open fork mount. The optical path of the light passing through the telescope is shown in Fig. 2.17. The incoming beam gets focused and reflected by the primary mirror towards a secondary mirror. There, it is reflected back to the primary mirror which has an opening in the middle through which the focused beam passes towards a detecting device (camera).

Figure 2.16: The 50 cm Cassegrain-telescope on the roof of the AIfA.

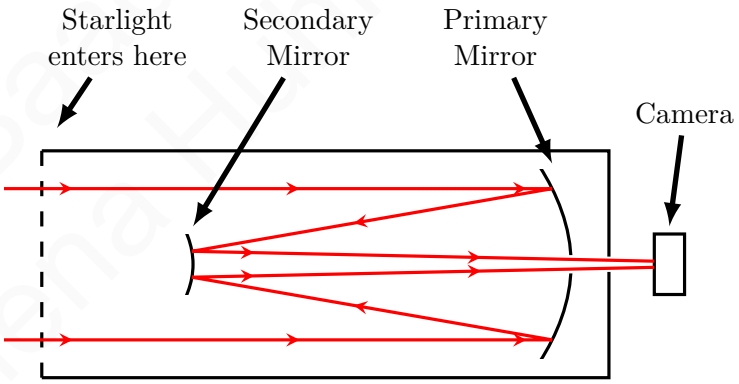

Figure 2.17: Optical path of a Cassegrain-telescope.

Chapter 3

Spectroscopy

This chapter summarizes the physics background needed for the laboratory course. The center of attention lies on the different line broadening mechanisms. The different mechanisms will be explained and it will be discussed what minimum values are needed for e.g. the rotational velocity, so that the line is broadened enough so it is possible to measure the broadening with the DADOS spectrograph.

3.1 The Doppler effect

The Doppler effect describes the change in frequency of a wave seen by an observer moving relative to the wave's source. The non-relativistic Doppler Equation, which can be used for velocities smaller than $1 \times 10^4\,\mathrm{km\,s^{-1}}$, is given by

$$\frac{\Delta\lambda}{\lambda} = \frac{v}{c} \quad , \tag{3.1}$$

where $\Delta\lambda$ is the observed wavelength shift due to the Doppler effect, λ is the wavelength of the wave at its source, v is the relative velocity between the source and observer, and c is the speed of light. All measured phenomena, observed by the students during the laboratory course, are due to the Doppler effect.

3.2 Line broadening mechanisms

Spectrophotometry refers to the study and application of line strengths and line profiles. Spectral lines contain more information than their wavelength alone, such as spectral line broadening due to stellar rotation or thermal motions within a star. Given the limitations of the instruments, and the required level of the laboratory course, in this thesis are only examined spectral linewidths and not their intensities.

In this section, the dominant line broadening mechanisms are summarized:

A spectral line that does not undergo line broadening is described by a Lorentzian

function. From Kitchin (1995):

$$I(\nu) = \frac{1}{\pi} \cdot \frac{\frac{\gamma}{2}}{(2\pi(\nu - \nu_0))^2 + \frac{\gamma}{2}^2} \quad ,$$

where $I(\nu)$ is the intensity of the spectral line at a given frequency ν, γ is the functions full-width-half-maximum and ν_0 is the central frequency of the line. Typical values of the natural linewidth are around $0.05\,\mathrm{km\,s^{-1}}$. It is not possible to measure linewidths this small with the DADOS spectrograph because of its limited resolution. Based on the natural linewidth, spectral lines can be broadened by different mechanisms. These are classified into two different types:

1. *Pressure broadened spectral lines*: Pressure broadening always happens when the density or, equivalently pressure, is high enough so that the mean time between two gas particle collisions is similar to the mean lifetime of the particles excited states. Because of this, the energy levels broaden (in the limiting case of a solid object, valence and conduction bands are built up). When rotational broadening can be neglected, pressure broadening is the dominant line broadening mechanism in stellar spectra. One can model the line profile of pressure broadened lines using a Lorentz profile.

2. *Doppler broadened spectral lines*: Doppler broadening occurs because of bulk motion of the matter within a star. It is due to, e.g. stellar rotation, binary stars, stellar winds and thermal and turbulent motions. The line profile of a Doppler-broadened line follows approximately a Gaussian profile. In this work are discussed the effects of Doppler broadening on stellar spectral lines; Pressure broadening is included for the sake of completeness.

The properties of stars that contribute most to line broadening are: 1.) stellar rotation (rotational broadening), 2.) Internal energy (thermal broadening), and 3.) Convection (or turbulent broadening).

The relevant physical constants are:

1. Speed of light $c = 299\,792\,458\,\mathrm{m\,s^{-1}}$

2. Boltzmann constant $k = 1.38 \times 10^{-23}\,\mathrm{J\,K^{-1}}$ and

3. Wavelength of $H\alpha = 6562.8\,\text{Å}$

All stars rotate. In most cases it is not possible to resolve the Doppler shifted lines. Instead, the combined light from parts of the star moving away from and towards the observer is measured. To determine the rotational velocity of a star from the broadening of its spectral lines, the method of Daflon et al. (2007) and Slettebak et al. (1975) was used. Daflon et al. and Slettebak et al. designed simulations to determine how much

the He I lines of an OB star broaden due to its intrinsic rotation. In their papers they displayed results in tabular form. After having measured the widths of the He I lines, one can easily look up the rotational velocity of the star being observed. For more details see Section 4.3.
Regulus is a prototype for a fast rotating (binary) star. According to SIMBAD[1] its rotational velocity is about $300\,\mathrm{km\,s^{-1}}$ and thus, with the given resolution, it is possible to measure the rotational broadening of Regulus with the DADOS spectrograph. See Section 4.3 for details.

Thermal broadening is due to the motion of the particles caused by the internal energy of the star. The line profile of an emission or absorption line of this type is described by the following equation from Kitchin (1995):

$$I(\lambda) = I(\lambda_0) e^{\frac{-mc^2(\lambda_0-\lambda)^2}{2kT\lambda^2}} \quad , \tag{3.2}$$

where $I(\lambda)$ is the intensity of the spectral line at wavelength λ, λ_0 is the wavelength emitted by the static atom, c the speed of light, k is the Boltzmann constant, T is the temperature of the star, and m is the mean molecular weight given by

$$m = \frac{1}{2x + \frac{3}{4}y + \frac{1}{2}z}\mathrm{u} \quad , \tag{3.3}$$

where x is the hydrogen fraction, y the helium fraction and z the fraction of metals in the outer layer of the star. For example for a star that consists of half hydrogen and half helium, $m = \frac{1}{2\cdot 0.5 + \frac{3}{4}\cdot 0.5 + \frac{1}{2}\cdot 0}\mathrm{u} = \frac{8}{11}\mathrm{u}$, where u is the atomic mass unit ($\mathrm{u} = 1.661 \times 10^{-27}\,\mathrm{kg}$) (Kippenhahn & Weigert 1990).
The full-width-half-maximum ($\Delta\lambda_{\frac{1}{2}}$) is calculated using

$$\Delta\lambda_{\frac{1}{2}} = \left(\frac{2kT\ln 2}{mc^2}\right)^{\frac{1}{2}} 2\lambda_0 \quad , \tag{3.4}$$

from Kitchin (1995). The line broadening due to turbulence (e.g. convection) can also be represented by a Gaussian line profile, as given by

$$I(\lambda) \approx I(\lambda_0) e^{\frac{-c^2(\lambda_0-\lambda)^2}{v^2\lambda_0^2}} \quad , \tag{3.5}$$

and the full-width-half-maximum can in this case be calculated using

$$\Delta\lambda_{\frac{1}{2}} = \left(\frac{v^2\ln 2}{c^2}\right)^{\frac{1}{2}} 2\lambda_0 \quad . \tag{3.6}$$

Here $I(\lambda)$ is the intensity of the spectral line at a given wavelength λ, λ_0 is the "natural" wavelength emitted by the static atom, c is the speed of light, and v is the characteristic velocity of the convective motion. Both equations are taken from Kitchin (1995). Table 3.1 lists the contributions of the various broadening mechanism to the total broadening of a spectral line for a typical B star with a temperature of 20 000 K, convective motions of $2\,\mathrm{km\,s^{-1}}$ and a rotational velocity of $200\,\mathrm{km\,s^{-1}}$.

[1] `http://simbad.u-strasbg.fr/simbad/`, accessed on August 29., 2011.

mechanism	**amount of property**	$\lambda_{\mathbf{broad}}$ / Å
rotational broadening	$200\,\mathrm{km\,s^{-1}}$	7.6
thermal broadening	20 000 K	0.8
turbulent broadening	$2\,\mathrm{km\,s^{-1}}$	0.07
natural linewidth	-	0.001

Table 3.1: The contributions λ_{broad} of rotational velocity, thermal broadening, turbulent broadening and natural linewidth to the total broadening of a spectral line for a typical B star with a temperature of 20 000 K, convective motions of $2\,\mathrm{km\,s^{-1}}$ and a rotational velocity of $200\,\mathrm{km\,s^{-1}}$. For the calculations of the individual contributions to the broadening it was assumed that all other contributions could be neglected.

Because of the limited resolution of the DADOS spectrograph, there is a lower limit of linewidths that can be observed. Every spectroscopic set-up has an intrinsic instrumental line profile with a given wavelength dependent width. Every observed stellar spectral line is convolved with this instrumental line profile and must always be corrected for it. The measured total width σ_{total} is thus composed of the instrumental profile width $\sigma_{\mathrm{instr.}}$ and the true stellar line width $\sigma_{\mathrm{stellar}}$. The linewidths of the two profiles are added in quadrature

$$\sigma_{\mathrm{total}} = \sqrt{\sigma^2_{\mathrm{instr.}} + \sigma^2_{\mathrm{stellar}}} \quad . \tag{3.7}$$

The wavelength dependent instrumental line profile can be obtained by measuring the widths of the spectral lines of the calibration lamp because the lines produced by the calibration lamp itself are so narrow that their widths can be neglected against the instrumental profile widths and so the measured widths represent the instrumental line profile. For this set-up, the widths of the instrumental line profile are listed in Table 2.1. To determine the statistical spread of the width of the instrumental line profile, the width of a (approximately 6900 Å) spectral line of the calibration lamp was measured in twelve different exposures with an exposure time of 0.5 s per frame. The results of this measurement were that the center of the line lied at $6965.38\,\text{Å} \pm 0.10\,\text{Å}$ and the linewidth was measured to be $1.95\,\text{Å} \pm 0.10\,\text{Å}$. The standard deviation of the linewidth and line center were determined to be approximately 0.03 Å. To be sure to have measured a true stellar linewidth and not just statistical fluctuations, a measured stellar linewidth needs to deviate more than instrumental linewidth plus three times the standard deviation from the instrumental profile. For this example that means that a measured stellar linewidth needs to be broader than $1.95\,\text{Å} + 0.10\,\text{Å} = 2.05\,\text{Å}$ so it can be said for sure that the broadening is due to physical processes in the star and not to any processes in the set-up

$$\sqrt{(1.95\,\text{Å})^2 + (\Delta\lambda_{\frac{1}{2}})^2} \overset{!}{>} 2.05\,\text{Å} \;\Rightarrow\; \Delta\lambda_{\frac{1}{2}} > 0.63\,\text{Å} \quad . \tag{3.8}$$

$\Delta\lambda_{\frac{1}{2}}$ can now be inserted in the previously described relations between linewidth and temperature, see Equation (3.4) and linewidth and convection velocity, see Equation (3.6). For the linewidth due to rotational velocity the threshold value of 2.05 Å must

be compared to the tables listed in Daflon et al. (2007) and Slettebak et al. (1975). Note that the values calculated above (and listed in Table 3.2) are the *most optimistic* estimates of what can be measured with the DADOS spectrograph.

Broadening mechanism	**Most optimistic estimate**
Rotational broadening	$100\,\mathrm{km\,s^{-1}}$
Temperature	$13\,000\,\mathrm{K}$
Convective velocity	$28\,\mathrm{km\,s^{-1}}$

Table 3.2: The *most optimistic* estimates for the accuracy of the rotational velocity, temperature and convection velocity that can be measured with the DADOS spectrograph. In each case it is assumed that the respective broadening mechanism dominates the others.

Chapter 4

Measurements and Results

In this Chapter the measurements made and results obtained will be presented. All data were reduced with IRAF and the linewidths were determined by fitting a Gaussian functions to the spectral lines. Methods of data reduction using IRAF are described in detail in Appendix B.

4.1 Overview

The main goal of this diploma thesis was to prepare a spectroscopy laboratory course for third year Bachelor students. After the equipment (see Chapter 2) was acquired, the first task was to determine the type of observations that can be carried out with the experimental setup. Because of the low resolution of the spectrograph, only a limited number of phenomena could be observed. Taking into account these hardware imposed limitations, a set of projects was defined which is appropriate for both the students' physics background, and the time allotted for this course in the physics/astronomy curriculum.

4.2 Binary stars

Most stars are found in some sort of binary system. A binary star system consists of two stars orbiting about a center of mass. From the observational point of view, several different types of binary systems exist. This laboratory course will be mainly concerned with spectroscopic binaries. Spectroscopic binaries are binary stars that can not be resolved visually. The evidence of being a binary star comes from the Doppler shift of the spectral lines. That means that the spectral lines of the stars show a periodic change in their position due to the Doppler effect. In case the spectral lines can not be resolved they show a periodic change in their widths. For more details read Section 4.2.1.

4.2.1 Determination of the total mass of a binary star system

In a binary system both stars orbit each other with their individual orbital velocities (v_1, v_2). These orbital velocities always need to be multiplied by a term $\sin i$, where i is the inclination angle. The factor $\sin i$ is needed because only projected velocities can be measured. For readability reasons, the term $\sin i$ is omitted in the whole chapter. Depending on the orbital phase of the star, the respective spectral lines are, due to the Doppler effect, either blue or red shifted. For this thesis the Hα line[1] was observed at a wavelength of 6562.8 Å. It is assumed that each stellar spectral line profile is described by a single Gaussian function. The chosen binary systems consist of two stars with the same spectral classes and **almost** the same magnitudes. The profiles describing spectral lines for each star individually can thus be assumed to have the same amplitudes $A_{1,2}$ and same widths $\sigma_{1,2}$. The variation of intensity of the Hα line with wavelength of star 1 of the binary system is thus described by

$$I_1(\lambda) = A_1 \cdot \frac{1}{\sigma_1\sqrt{2\pi}} \cdot \exp\left(-\frac{(\lambda - 6562.8\,\text{Å} - \mu_1)^2}{2\sigma_1^2}\right) \quad ,$$

and of star 2 by

$$I_2(\lambda) = A_2 \cdot \frac{1}{\sigma_2\sqrt{2\pi}} \cdot \exp\left(-\frac{(\lambda - 6562.8\,\text{Å} - \mu_2)^2}{2\sigma_2^2}\right) \quad .$$

Here λ is the wavelength, $I_{1,2}$ are the respective intensities of the lines, $A_{1,2}$ are the respective amplitudes, $\sigma_{1,2}$ are the respective widths and $\mu_{1,2}$ represent the shift of the total line compared to the rest wavelength at 6562.8 Å. There are two extreme cases:

1. The two stars stand behind each other (from the observers point of view. See Fig. 4.1.a) and there is thus no resulting radial velocity (no Doppler shifted lines). The observer sees just one Hα line, which is the sum of the two individual Hα lines of the two stars with a total width of $\sigma_1 = \sigma_2 = \sigma_0$. This case from now on will be referred to as the *zero shift position* $\Rightarrow \mu_1 = \mu_2 = 0$.

2. The two stars stand side by side (from the observers point of view. See Fig. 4.1.b). This is the configuration with maximum radial velocity and thus maximum Doppler shifted lines. The linewidth is at maximum $\sigma_{\max}$. This case from now on will be referred to as the *maximum separation position* $\Rightarrow |\mu_1| + |\mu_2| = \mu_{\text{tot}} = \text{maximal}$.

Figure 4.1 shows the position of the spectral lines according to the orbital phase of the stars. Because of the limited resolution of the spectrograph, the two components can not be resolved individually. The observer just sees a periodic change between a smaller spectral line with linewidth σ_0 (at zero shift position) and a broader spectral

[1] It was decided to use the Hα line for the observations because first, the resolution of the DADOS spectrograph was best around 6000 Å and second, the quantum efficiency of the camera was best around 6000 Å.

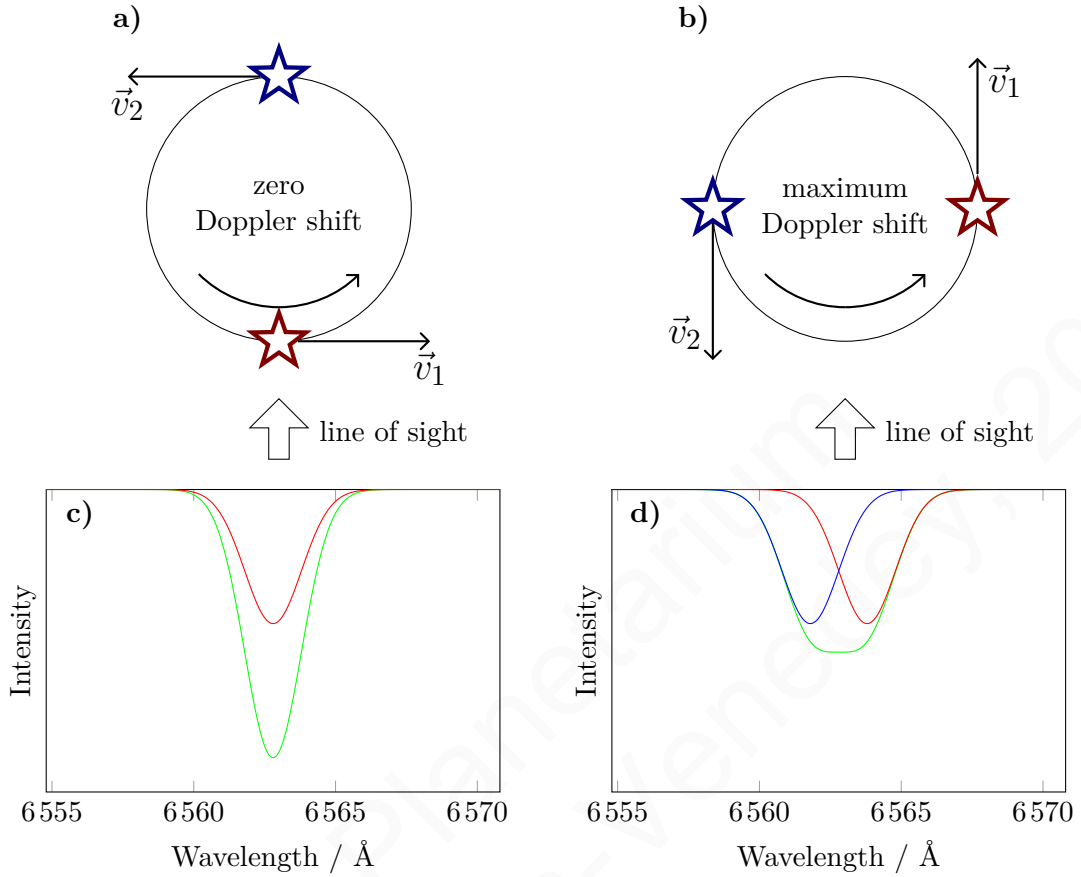

Figure 4.1: Depending on the orbital phase and direction of motion of the stars, the spectral lines are either blue- or red-shifted. The broad arrows in Fig. **a** and **b** indicate the line of sight. The red curve shows the sum of the respective two spectral lines (here was chosen the Hα line at 6562.8 Å). In Fig. **c** there is no shift due to the Doppler effect (zero shift); Fig. **d** shows an example for the maximum Doppler shift (maximum separation). In this example the two shifted spectral lines cannot be resolved, the width of the spectral line representing the sum in Fig. **d** is just broader compared to the width of the spectral line representing the sum in Fig. **c**.

line with linewidth $\sigma_{\max}$ (at maximum separation position). Although μ_1 and μ_2 can not be determined individually, μ_{tot}, which is proportional to the sum of the two orbital velocities of the binary system, can. From now on the sum of the two orbital velocities will be referred to as the *total orbital velocity*. With Kepler's laws the total orbital velocity of the system can be converted to the total mass of the system. The following procedure was used to determine μ_{tot}:

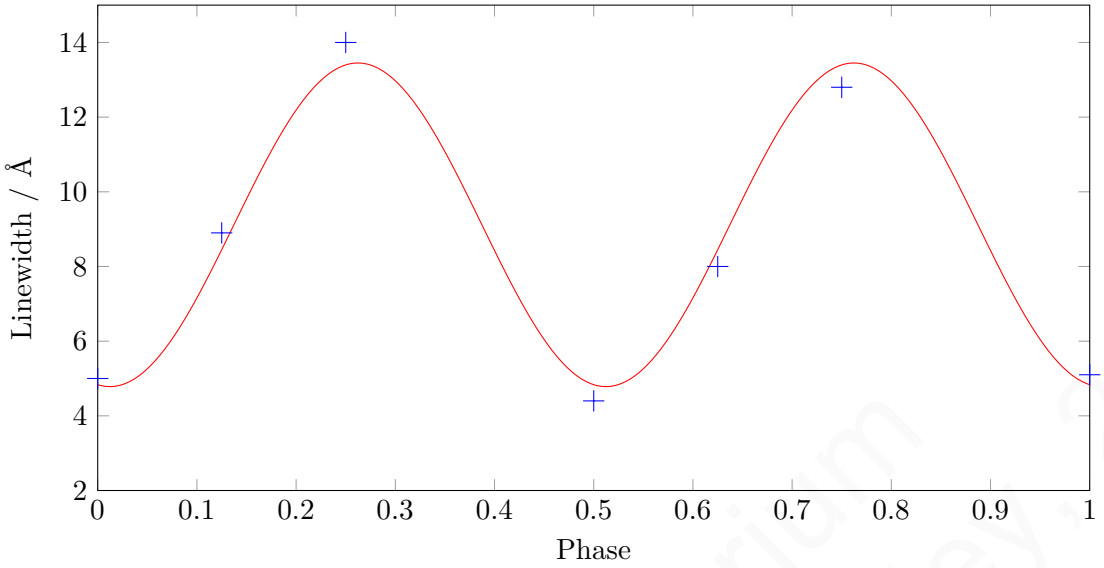

Figure 4.2: An example of the periodic change of an observed linewidth of a spectral line of a binary star system, where the components can not be resolved individually. The function describing the change is a sine. The data points are artificially generated for demonstrative purposes. The epochs and the periods of the binary systems are known, thus the phase can be calculated precisely and is not a free parameter of the fit.

The binary system was observed for different points in time. It was paid attention that the observations were covering the whole cycle. The epochs[2] and periods of the binary systems are known from Batten et al. (1989). The data were reduced and the widths of the Hα line were determined. The phase at which the image frames were taken was calculated taking into account the periodic circulation of the stars. The plot of phase vs. linewidth reflects the periodicity of the linewidth with the orbital phase. Between phase 0 and 1 the system runs through two maximum separation positions and two zero shift positions. For both systems, observed for this diploma thesis, it was assumed that both stars move on a perfect circular path, thus the function describing the relationship between the linewidth and the phase of the system, was a sine. The following function was fit to the observed data,

$$f(x) = a\sin(4\pi \cdot x - c) + d \quad , \tag{4.1}$$

where a represents the amplitude of the sine, c the left-right shift and d the offset. Figure 4.2 shows exemplarily the periodic change in the width. The phase can be calculated precisely and is not a free parameter of the fit. The desired quantity is the shift μ_{tot} between the centers of the two Gaussian functions of equal amplitude. The following simulation is carried out in order to translate the width of the observed line to the separation of the two underlying components.

[2]Date and time of a zero shift culmination, given in modified Julian date.

- The minimum broadening full-width-half-maximum measured at zero shift position, σ_0, gives the width of the single components to be used.

- Two Gaussian functions (of equal amplitude and full-width-half-maxima, and centers at 6562.8 Å are now progressively shifted, so that $|\mu_2| = |\mu_1|$ (μ_1 and μ_2 always have opposed algebraic signs).

- The width of the *sum* of these Gaussian functions is the equivalent of the full-width-half-maximum observed at different orbital phases.

- The full-width-half-maximum of this sum is determined and plotted as a function of the shift.

- Thus, using this plot for a known minimum broadening full-width-half-maximum, σ_0, the measured width at maximum separation position, $\sigma_{\max}$, can be read off the plot and thus translated into the shift, $\mu_{\max}$, between the two Gaussian functions. This shift can be converted into the total orbital velocity by using the Doppler Equation (3.1).

The course of the width was simulated for different minimum broadening full-width-half-maxima. Figure 4.3 shows three examples for minimum widths of 1.5 Å, 2.5 Å and 4.5 Å. The mass of the system can be calculated using the following equations. According to $s = v \cdot t$ (where s is the distance, v the velocity and t the time) follows:

$$a_{tot} = a_1 + a_2 = \frac{P}{2\pi} v_{\text{tot}} \quad , \tag{4.2}$$

where $a_{\text{tot}} = a_1 + a_2$ is the major axis of the system, $a_{1,2}$ are the distances between the center of mass and the components of the binary system (see Fig. 4.4), P is the period of the system and v_{tot} is the total orbital velocity determined above. Using Kepler's law the total mass, m_{tot}, of the system is:

$$m_{\text{tot}} = m_1 + m_2 = \frac{a_{\text{tot}}^3}{P^2} \frac{4\pi^2}{G} \quad , \tag{4.3}$$

where $m_{1,2}$ are the individual masses of the stars and G is the gravitational constant. The error on m_{tot} is calculated according to standard error propagation:

$$\Delta m_{\text{tot}} = \sqrt{\left(\frac{\partial m_{\text{tot}}}{\partial a_{\text{tot}}} \Delta a_{\text{tot}} \right)^2} = \frac{6\pi a_{\text{tot}}^2}{PG} \Delta v_{\text{tot}} \quad , \tag{4.4}$$

where Δm_{tot} is the error on m_{tot} and Δv_{tot} is the error on the total orbital velocity of the system. Δv_{tot} is determined graphically for each system. See sections 4.2.2 and 4.2.3 respectively.

Two systems are especially qualified for being observed because of their *short periods*, their *high orbital velocities* and the fact that both components of each system have the

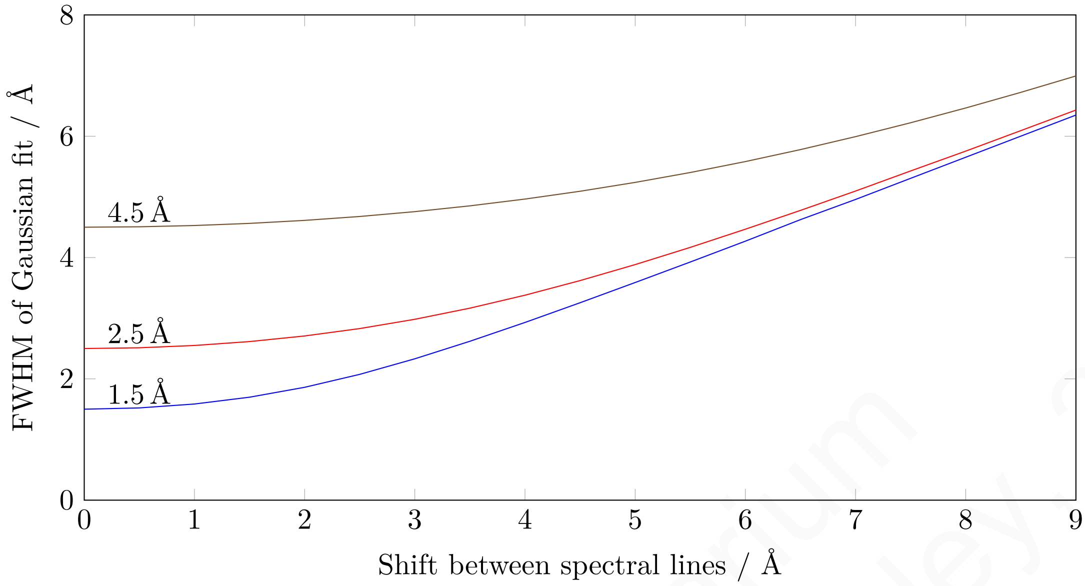

Figure 4.3: Course of the full-width-half-maximum of a stellar spectral line of a binary star system where the two components of the line can not be resolved individually. The greater the shift between the two components, the broader the linewidth. Here it was simulated for three different values of the minimum broadening full-width-half-maximum, σ_0, 1.5 Å, 2.5 Å and 4.5 Å. It is assumed that both single spectral lines have the same width and same amplitude, because they are produced by stars of the same spectral class and almost the same magnitude.

same spectral class and **nearly** the same magnitude. Thus the spectral lines produced by the stars of each system can be **assumed** to have the *same width* and *same intensity*. Table 4.1 names the two systems and lists, briefly, their properties which are important for this laboratory course. The students have to measure the periodic change of the linewidths and, thus, need to measure the linewidths at different points in time. Short periods are desired because the measurement should take place during one night. The whole cycle should be measured and the data points should be numerous and evenly distributed. The chosen systems have high orbital velocities, but these are insufficient for the spectral lines to clearly separate. The higher the orbital velocity of the system, the bigger the shift between the two spectral lines and, thus, the broader the width of the spectral line.

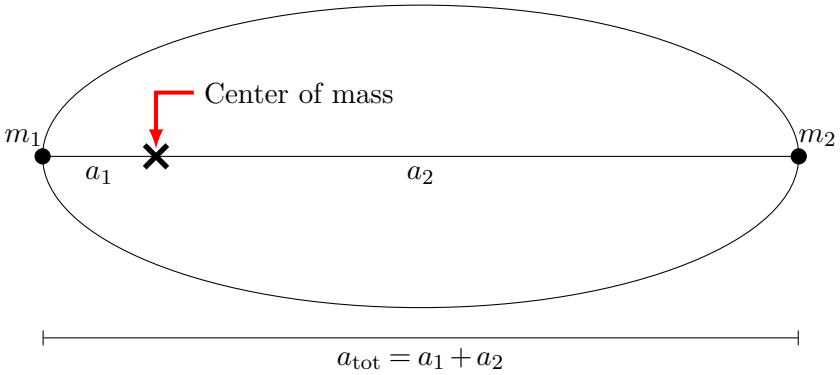

Figure 4.4: Schematic of a stellar binary system orbiting a common center of mass. $a_{1,2}$ are the distances between the center of mass, and the components of the system.

Property	**44 Boötis**		**AO Cassiopeiae**	
Coordinates (ICRS (J2000))	RA 15 03 47.29565		RA 00 17 43.06183	
	DEC +47 39 14.6228		DEC +51 25 59.1242	
Period	0.267 818 d		3.523 487 d	
Epoch (MJD)	28 635.368		35 957.058	
V-Magnitude	6.1	6.55	6.09	6.24
Orbital Velocity	115.4 km s^{-1}	231.1 km s^{-1}	223.4 km s^{-1}	174.8 km s^{-1}
Spectral class	G 2V	G 2V	O 9III	O 9III

Table 4.1: Properties of two binary systems (44 Boötis, AO Cassiopeiae) which are well suited for the demands of the laboratory course. All properties are taken from Batten et al. (1989), only the coordinates are taken from `http://simbad.u-strasbg.fr/simbad/`, accessed on August 29., 2011.

4.2.2 Measurement of 44 Boötis

44 Boötis is a binary star system of two G 2V stars with magnitudes $V = 6.1$ mag and $V = 6.55$ mag and a period of 0.267 818 d. Furthermore this system has a very high total orbital velocity, namely $115.4\,\mathrm{km\,s^{-1}} + 231.1\,\mathrm{km\,s^{-1}} = 346.5\,\mathrm{km\,s^{-1}}$, from Batten et al. (1989). Figure 4.5 is an example of one of the frames used for the determination of the total orbital velocity (sum of the orbital velocities of the two stars) and thus to calculate the total mass of the system. The data were taken on different nights, see Table 4.2 for the listed object frames. Figure 4.6 shows the measured data points together with an error weighted sine fit, Equation (4.1), used to determine the minimum broadening full-width-half-maximum, σ_0, and the width at maximum separation, σ_{max}, of the Hα line. The fit parameters are given in Table 4.3. The uncertainty on one data point was determined by calculating a phase dependent standard deviation. If a width is determined several times for the same phase, it is expected that, for each measurement,

Name of frame	Phase	FWHM of Hα / Å
obj00209	0.292	12.36
obj00221	0.494	6.30
obj00227	0.752	10.12
obj00231	0.011	6.08
obj00248	0.484	6.09
obj00254	0.857	10.67
obj00258	0.998	7.02
obj00260	0.125	10.42
obj00261	0.250	12.72
obj00263	0.375	11.26
obj00266	0.501	8.04
obj00271	0.625	10.18
obj00272	0.731	11.05
obj00275	0.130	10.13

Table 4.2: Object frames of 44 Boötis used for the determination of the total orbital velocity and thus the total mass of the system. The phase was calculated precisely with the information of epoch, period and observing time. The full-width-half maxima were measured with IRAF.

Amplitude a	Left-right shift c	Offset d	Minimum	Maximum
2.63	1.63	9.92	7.3 Å	12.6 Å

Table 4.3: Parameters of the sine fit to the observed data of 44 Boötis. a represents the amplitude of the sine, c the left-right shift and d the offset. Thus $d-a$ equals the minimum of the sine and $d+a$ represents the maximum.

the width should stay the same. The deviation gives the uncertainty on the measured width for the different orbital phases and, thus, each data point is afflicted with this calculated phase dependent uncertainty.

In the data a minimum broadening width of $7.3\,\text{Å} \pm 0.8\,\text{Å}$ was read off the sine fit. With this value a simulation can be done; Figure 4.7 shows the simulated course of the width for 44 Boötis. The width at maximum separation was determined to be $12.6\,\text{Å} \pm 1.1\,\text{Å}$. The shift corresponding to this value can be read off the simulated plot (Fig. 4.7) and is 7.1 Å, corresponding to a total orbital velocity of $320\,\text{km}\,\text{s}^{-1}$, converted with the Doppler Equation (3.1). The error estimation is done graphically, which is justifiable because the linewidth as a function of spectral line shift is linear in the region of interest, as can be seen in Fig. 4.8. The error determined in this way is $40\,\text{km}\,\text{s}^{-1}$.

The total orbital velocity of 44 Boötis is $320\,\text{km}\,\text{s}^{-1} \pm 40\,\text{km}\,\text{s}^{-1}$.

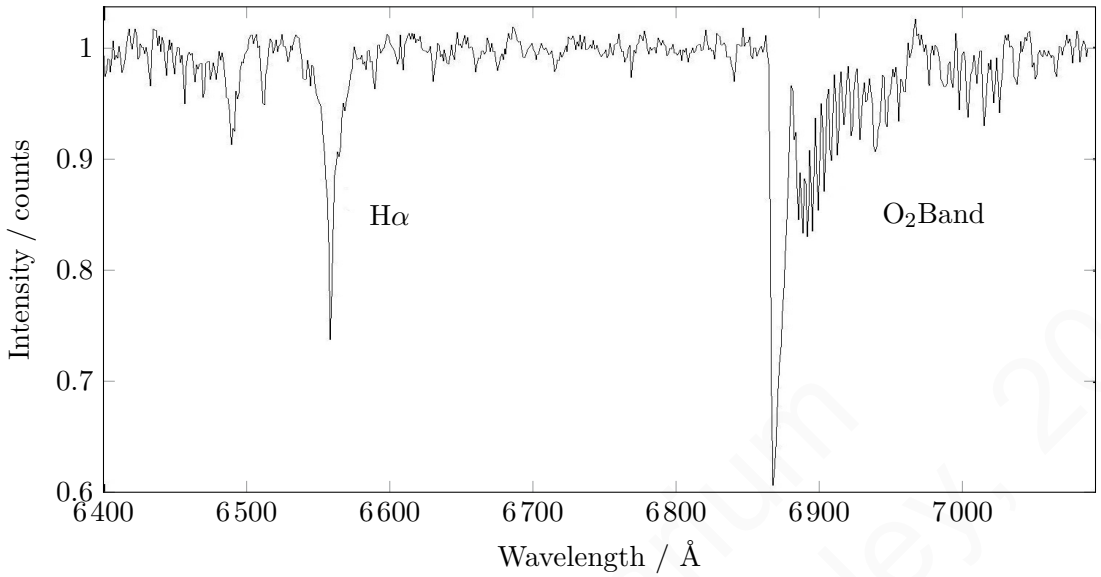

Figure 4.5: Spectrum of 44 Boötis. The spectral line on the left hand side is Hα; the one on the right hand side is the atmospheric O_2 B Band.

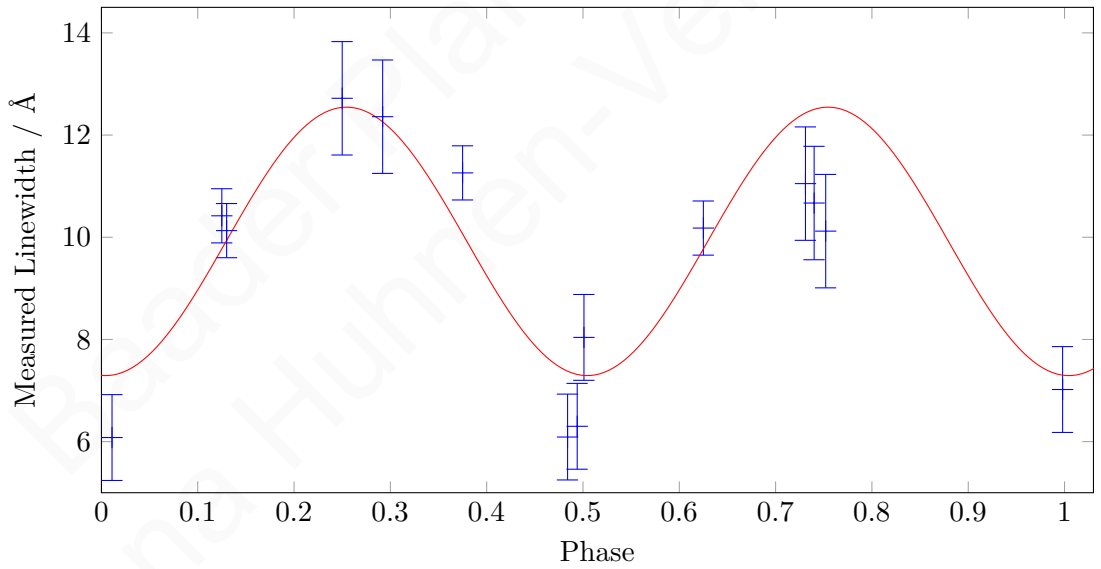

Figure 4.6: Error weighted sine, fit to the observed linewidths of Hα of 44 Boötis. Fitting parameters were amplitude, left-right shift and offset. The period was not a free parameter. The minimum value of the fit was $7.3\,\text{Å} \pm 0.8\,\text{Å}$; the maximum value was $12.6\,\text{Å} \pm 1.1\,\text{Å}$. These values were now used for the simulation to find the shift between the two spectral lines for the determination of the total orbital velocity of the system of 44 Boötis.

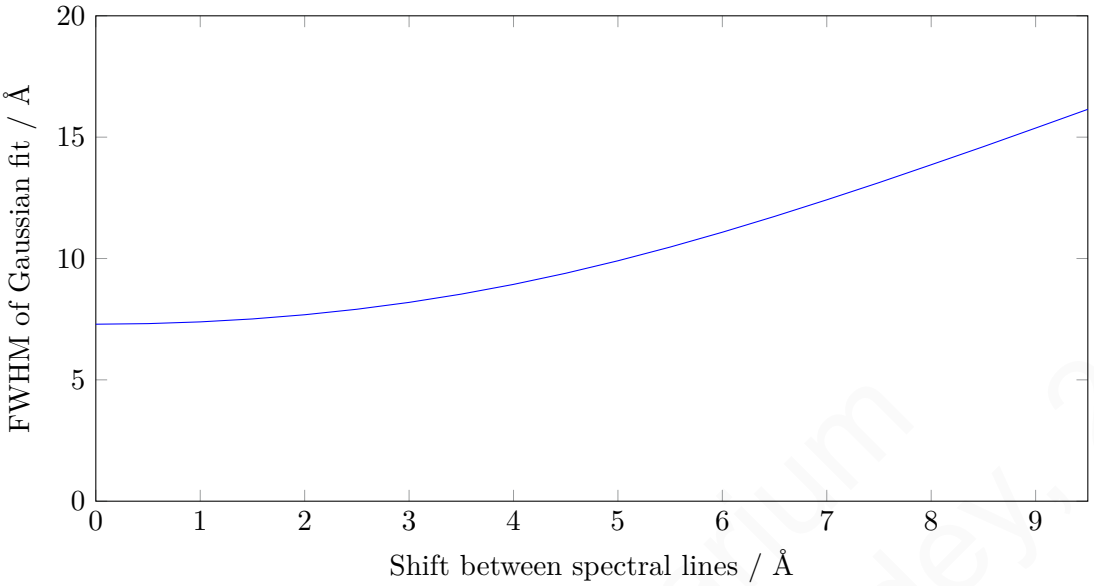

Figure 4.7: Simulated linewidth as a function of spectral line shift for 44 Boötis with a minimum broadening width, σ_0, of 7.3 Å. The width of the Hα line of 44 Boötis at maximum separation was 12.6 Å. The shift corresponding to this value could be read off this simulated plot and was 7.1 Å.

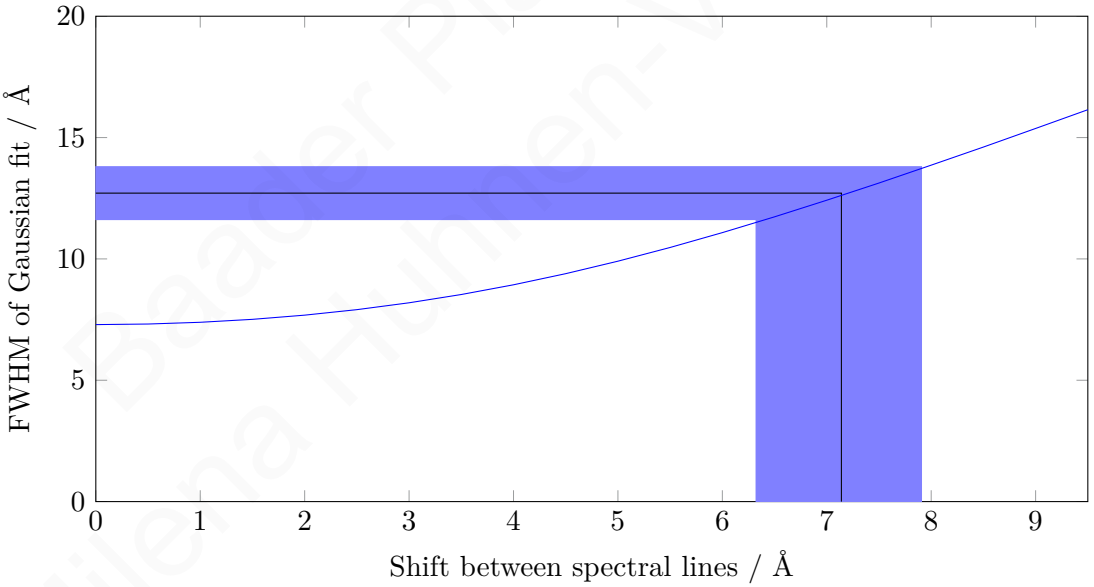

Figure 4.8: The linewidth as a function of spectral line shift is linear in the region of interest so it is justifiable to determine the error graphically (standard error propagation). The error on the total orbital velocity of 44 Boötis was determined to be 40 km s^{-1}.

With this information it is possible to estimate the system's total mass with Equations (4.2), (4.3) and (4.4):

The total mass of the system of 44 Boötis is $1.0\,M_\odot \pm 0.3\,M_\odot$

The spectroscopic binary catalog (Batten et al. 1989) lists 44 Boötis (entry 826) with a total orbital velocity of $115.4\,\mathrm{km\,s^{-1}} + 231.1\,\mathrm{km\,s^{-1}} = 346.5\,\mathrm{km\,s^{-1}}$. This corresponds to a total mass of the system of $1.16\,M_\odot$. Both values obtained here thus agree, within the estimated errors, with the published results in Batten et al. (1989).

4.2.3 Measurement of AO Cassiopeiae

AO Cassiopeiae is a binary star system consisting of two O 9III stars with magnitudes $V = 6.09\,\mathrm{mag}$ and $V = 6.24\,\mathrm{mag}$; the period is 3.523 487 d (Batten et al. 1989); the total orbital velocity, $223.4\,\mathrm{km\,s^{-1}} + 174.8\,\mathrm{km\,s^{-1}} = 398.2\,\mathrm{km\,s^{-1}}$, is even higher than that of 44 Boötis. Again, the measurements were made with the Hα line. Because of the longer period of AO Cassiopeiae it was more difficult to obtain desired measurements at the desired phases. Figure 4.9 shows two spectra of AO Cassiopeiae. One is taken at a phase of 0.476 (approximately zero shift) and one at a phase of 0.219 (approximately maximum separation). Because of the higher orbital velocity of AO Cassiopeiae compared to 44 Boötis, the shift between the two components of the Hα line is large enough so that even with the limited resolution of the DADOS spectrograph hints of the splitting can be seen. The Hα line in the spectrum on the right (in Fig. 4.9) has approximately half the intensity of the one on the left and the splitting starts at the tip of the line. All stellar lines of AO Cassiopeiae show the periodic change of the linewidth due to the Doppler effect. In this example, one clearly sees that the telluric O_2 line stays the same but the stellar C I line at 6672.94 Å also gets less intense and starts to split. At this point, the faint line to the left of the Hα cannot be identified but, like the O_2 line, it does not change its appearance. The data used for the determination of the total mass of the system was taken in different nights. Table 4.4 lists the frames used for the calculation of the orbital velocity. The data were evaluated in the same manner as that of 44 Boötis. Figure 4.10 shows the measured data points together with an error weighted sine fit used to determine the zero shift width, σ_0, and maximum separation width, $\sigma_{\max}$, of the Hα line. Again, the uncertainty on one data point was determined by calculating a phase dependent standard deviation. It is assumed that all measured widths at zero shift position should be the same. Reality is that they are not, so it must be assumed that each data point is afflicted with the aforementioned uncertainty. From the data a zero shift width of $2.9\,\text{Å} \pm 0.5\,\text{Å}$ was read off the sine fit. With this value the simulation could be done. Figure 4.11 shows the simulated course of the width for AO Cassiopeiae. The width at maximum position was determined to be $14.6\,\text{Å} \pm 0.3\,\text{Å}$; the shift corresponding to this value can be read off the simulated plot and was 8.7 Å. This

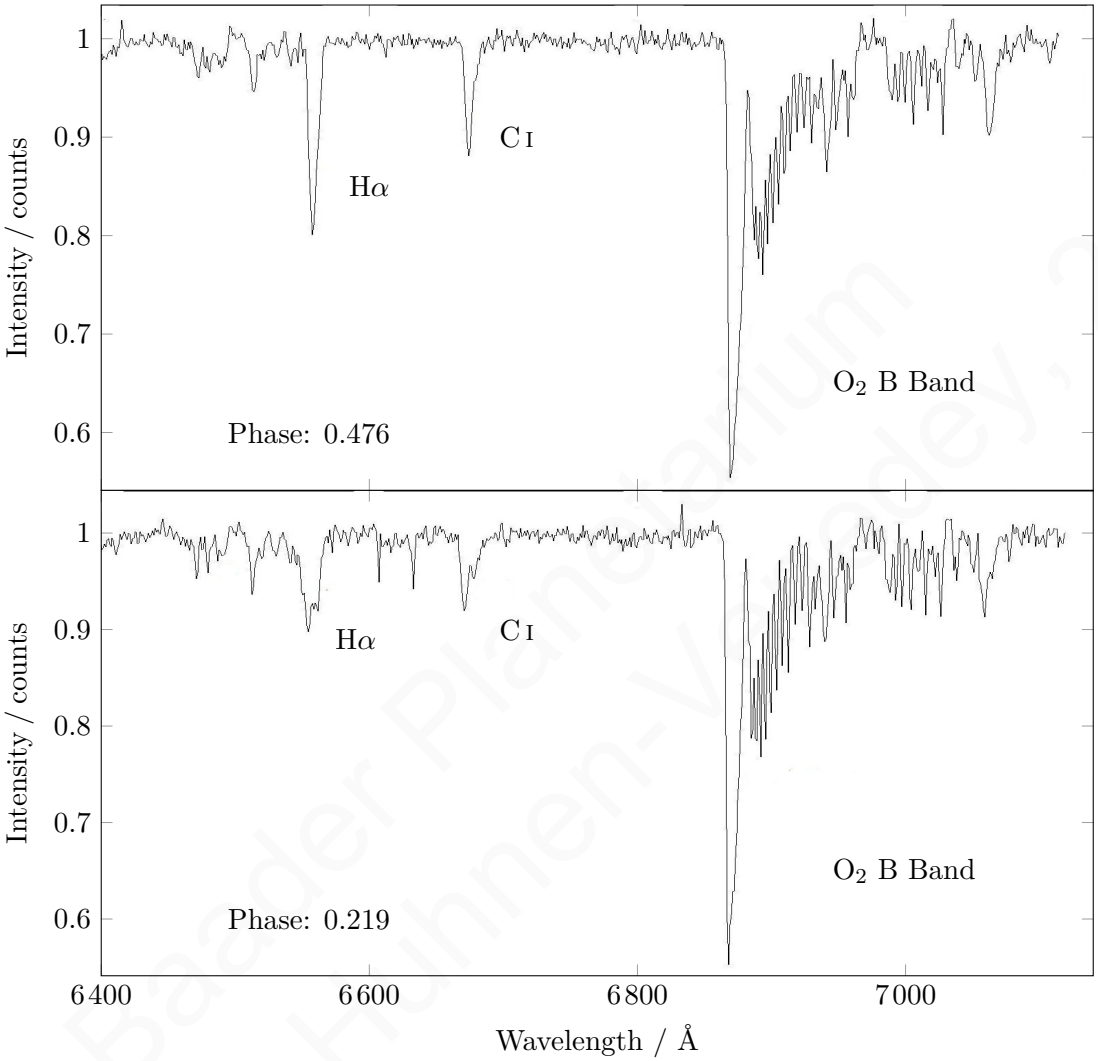

Figure 4.9: Spectra of AO Cassiopeiae at two different phases (0.476 and 0.219) taken with the DADOS spectrograph and the AIfA 50 cm-telescope. At maximum separation the stellar lines began to split, as can be seen in the spectrum to the right. Telluric lines such as as the O_2 line, are not affected by the orbital motion of the stars. The unidentified line to the left of Hα does not show any effect either, suggesting that is is not a stellar line of AO Cassiopeiae.

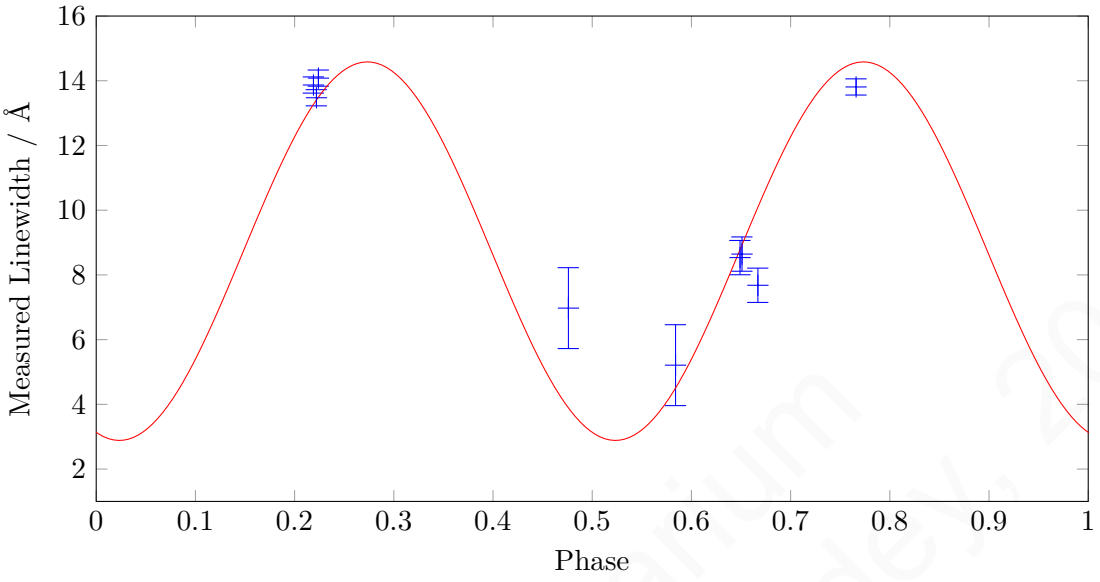

Figure 4.10: Error weighted sine fit to measured linewidths of Hα of AO Cassiopeiae, fitting parameters are amplitude, left-right shift and offset. The period is not a free parameter. The zero shift width, σ_0, and maximum separation width, $\sigma_{\max}$ could be read off the plot; and were 2.9 Å and 14.6 Å respectively.

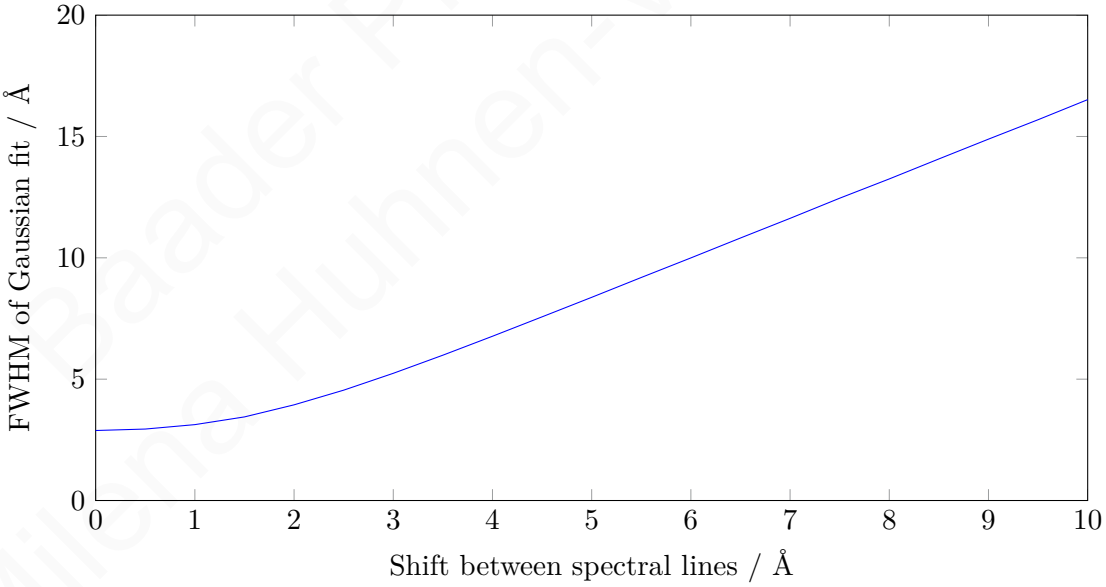

Figure 4.11: Simulated linewidth as a function of spectral line shift for AO Cassiopeiae with a minimum broadening width, σ_0, of 2.9 Å. The width of the Hα line of AO Cassiopeiae at maximum separation, $\sigma_{\max}$, was 14.6 Å.

Name of frame	**Phase**	**FWHM of Hα / Å**
obj00223	0.649	8.54
obj00224	0.651	8.64
obj00226	0.667	7.68
obj00232	0.219	13.87
obj00233	0.222	13.48
obj00234	0.224	14.08
obj00250	0.766	13.81
obj00264	0.476	6.97
obj00277	0.584	5.21

Table 4.4: Object frames of AO Cassiopeiae used for the determination of the total mass of the system. The data were taken on different nights. Because of the longer period of AO Cassiopeiae of about 3.5 d, it was more difficult to observe the desired phases compared to 44 Boötis, which has a period of only about 6.5 h.

Amplitude a	**Left-right shift c**	**Offset d**	**Minimum**	**Maximum**
5.85	1.69	8.73	2.9 Å	14.6 Å

Table 4.5: Parameters of the sine fit to the observed data of AO Cassiopeiae. a represents the amplitude of the sine, c the left-right shift and d the offset. Thus $d-a$ equals the minimum of the sine and $d+a$ is the maximum.

equates to a total orbital velocity of $399\,\mathrm{km\,s^{-1}}$. As for 44 Boötis the error estimation was done graphically, which was justifiable since the linewidth as a function of spectral line shift is linear in the region of interest, as can be seen in Fig. 4.12. The determined error was $8\,\mathrm{km\,s^{-1}}$.

The total orbital velocity of AO Cassiopeiae is $399\,\mathrm{km\,s^{-1}} \pm 8\,\mathrm{km\,s^{-1}}$.

With the same equations as for 44 Boötis the total mass of the system was calculated:

The total mass of the system of AO Cassiopeiae is $23\,\mathrm{M_\odot} \pm 1.5\,\mathrm{M_\odot}$

The spectroscopic binary catalog (Batten et al. 1989) lists AO Cassiopeiae (entry 12) with an total orbital velocity of $223.4\,\mathrm{km\,s^{-1}} + 174.8\,\mathrm{km\,s^{-1}} = 398.2\,\mathrm{km\,s^{-1}}$. This corresponds to a total mass of the system of $23\,\mathrm{M_\odot}$. Again, the measured values agree within the errors with the accepted ones of Batten et al. (1989).

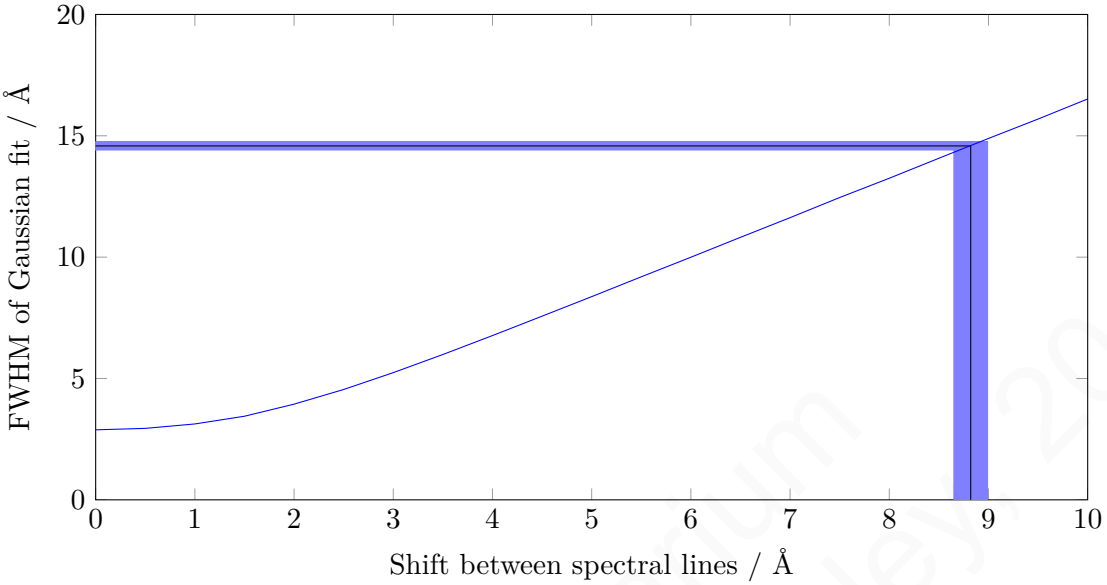

Figure 4.12: The linewidth as a function of spectral line shift is linear in the region of interest so it was justifiable to determine the error graphically (standard error propagation). The so determined error on the total orbital velocity of AO Cassiopeiae was $8\,\mathrm{km\,s^{-1}}$.

4.2.4 Conclusions

For both systems the results were consistent within the errors with published values (Batten et al. 1989). This leads to the conclusion that methods outlined here were correct and lead to accurate results in spite of the assumptions that were made. The inclination angle, i, is not taken into account, so all results must be multiplied by $\sin i$. Because of limited observing time, the students can not take as many data points as were used for this diploma thesis. The period and epoch of the eclipses (epoch = time of zero shift passage) are known, from Batten et al. (1989), so the students can calculate in advance the time periods for zero shift and maximum separation of the spectral lines and thus can coordinate their measurements to get these values. There is no need of a full cycle measurement of the binary systems. The problem with AO Cassiopeiae is that it has a period longer than one night. This makes it more difficult to obtain data at the desired phases. As can be seen if one compares Fig. 4.6 to Fig. 4.10, the available data on AO Cassiopeiae are rather meager. So it is important for further observations to get more data of AO Cassiopeiae to verify the result.

4.3 Determination of the projected rotational velocity of Regulus

During the laboratory course the students will also determine the rotational velocity of a star. They may choose which star they want to observe but have to motivate and explain their decision. It is advisable to observe B-type stars because the distribution of projected rotational velocities ($v \sin i$) of stars as a function of spectral type shows that the B-type stars have the largest average $v \sin i$ values among all main-sequence stars (Daflon et al. 2007).

4.3.1 Measurements

One way to determine the projected rotational velocities for O and B stars is to rely on a procedure described by Daflon et al. (2007) and Slettebak et al. (1975).

"An approach that is frequently employed in order to obtain estimates of the projected rotational velocity consists of measuring the full-width-half-maxima of He I lines and adopting relationships between full-width-half-maximum and $v \sin i$ established from observational data such as given by Slettebak et al. (1975). Alternatively, the projected rotational speed can be obtained from the comparison between observational and synthetic profiles of helium and metallic lines. By Daflon et al., a grid of synthetic spectra of He I line profiles was calculated in non local thermodynamic equilibrium using an extensive helium model atom and updatet atomic data. The synthetic spectra were computed using the codes DETAIL (Giddings 1981) and SURFACE (Butler & Giddings 1985) plus line-blanketed local thermodynamic equilibrium ATLAS9 model atmospheres (Kurucz 1993)". Text copied from Daflon et al. (2007).

Daflon et al. provide tables with full-width-half-maxima (in Å) of theoretical He profiles for OB stars with different temperatures (see Tables 4.6a to 4.6d).

The width of a line of the calibration lamp at approximately 4300 Å was approximately 1.67 Å. As already mentioned in Section 3.2 the widths of the spectral lines of the calibration lamp represent the linewidth of the instrumental profile. The most optimistic estimate for the linewidth of a real signal measured around approximately 4300 Å is the width of the instrumental profile, 1.67 Å, plus the 3σ error of the measured widths of the instrumental profile, 0.1 Å, thus 1.68 Å. This was the minimum width that must be observed in order to be sure that not only the width of the instrumental line profile alone was measured. One must take care that if a linewidth of a He I line was measured, the width of the instrumental profile (1.67 Å) must be corrected according to Equation (3.7) before the resulting width could be compared to the values in Tables 4.6a to 4.6d. Because of this, and to be sure that only line broadening due to rotation is measured, it is advisable that the students choose stars that rotate with a rotational velocity of at least 150 $\mathrm{km\,s^{-1}}$ to determine the rotational velocity. As an example in this diploma

v sin i / $\mathrm{km\,s^{-1}}$	λ_1/Å	λ_2/Å	λ_3/Å
0	1.04	1.02	0.65
50	2.01	1.90	1.59
100	3.01	2.86	3.03
150	4.10	3.92	4.38
200	5.11	4.94	5.49
250	6.05	6.02	6.55
300	7.01	7.34	7.61
350	7.99	8.51	8.66
400	8.99	9.64	9.77

(a) $T_{\mathrm{eff}} = 15000\,\mathrm{K}$

v sin i / $\mathrm{km\,s^{-1}}$	λ_1/Å	λ_2/Å	λ_3/Å
0	1.74	0.99	1.09
50	2.54	1.89	1.93
100	3.43	2.82	3.42
150	4.25	3.84	4.53
200	5.08	4.92	5.49
250	5.98	6.07	6.51
300	6.92	7.22	7.55
350	7.90	8.36	8.60
400	8.87	9.48	9.68

(b) $T_{\mathrm{eff}} = 20000\,\mathrm{K}$

v sin i / $\mathrm{km\,s^{-1}}$	λ_1/Å	λ_2/Å	λ_3/Å
0	1.55	0.91	1.06
50	2.30	1.74	1.82
100	3.16	2.70	3.25
150	4.01	3.73	4.31
200	4.87	4.81	5.31
250	5.79	5.95	6.33
300	6.74	7.12	7.37
350	7.71	8.25	8.45
400	8.71	9.36	9.54

(c) $T_{\mathrm{eff}} = 25000\,\mathrm{K}$

v sin i / $\mathrm{km\,s^{-1}}$	λ_1/Å	λ_2/Å	λ_3/Å
0	1.44	0.86	1.05
50	2.08	1.63	1.69
100	2.91	2.59	3.07
150	3.80	3.63	4.11
200	4.71	4.71	5.13
250	5.65	5.86	6.18
300	6.63	7.00	7.22
350	7.62	8.14	8.32
400	8.65	9.27	9.42

(d) $T_{\mathrm{eff}} = 30000\,\mathrm{K}$

Table 4.6: The full-width-half-maximum of theoretical He I profiles for different temperatures T and different transitions of He I with $\lambda_1 = 4026\,\text{Å}$, $\lambda_2 = 4388\,\text{Å}$ and $\lambda_3 = 4471\,\text{Å}$. From Daflon et al. (2007).

thesis, the rotational velocity of Regulus was measured. Regulus is a fast rotating and very bright star (bright means better signal-to-noise ratio). The spectrum of Regulus is shown in Fig. 4.13. Regulus is a B 7V star with a surface temperature of about 15000 K.[3] Thus the theoretical linewidths in Table 4.6a apply (see also Figs. 4.14 to 4.14). For clarity, the data in Table 4.6a was plotted and a linear fit ($f(x) = mx + b$) was performed (see Fig. 4.14). Table 4.7 lists the parameters (slope m and offset b) of the fits. To compare the measured linewidths to the values from Daflon et al., the measured full-width-half-maxima of the He I linewidths were entered into the equations of the linear fits. Table 4.8 displays the results. To get the rotational velocity of Regulus, the three values had to be averaged, see (Daflon et al. 2007) and (Slettebak et al. 1975) for details. The determined projected rotational velocity for Regulus was $290\,\mathrm{km\,s^{-1}}$.

[3] From `http://en.wikipedia.org/wiki/Spectral_class`, accessed on August 29., 2011.

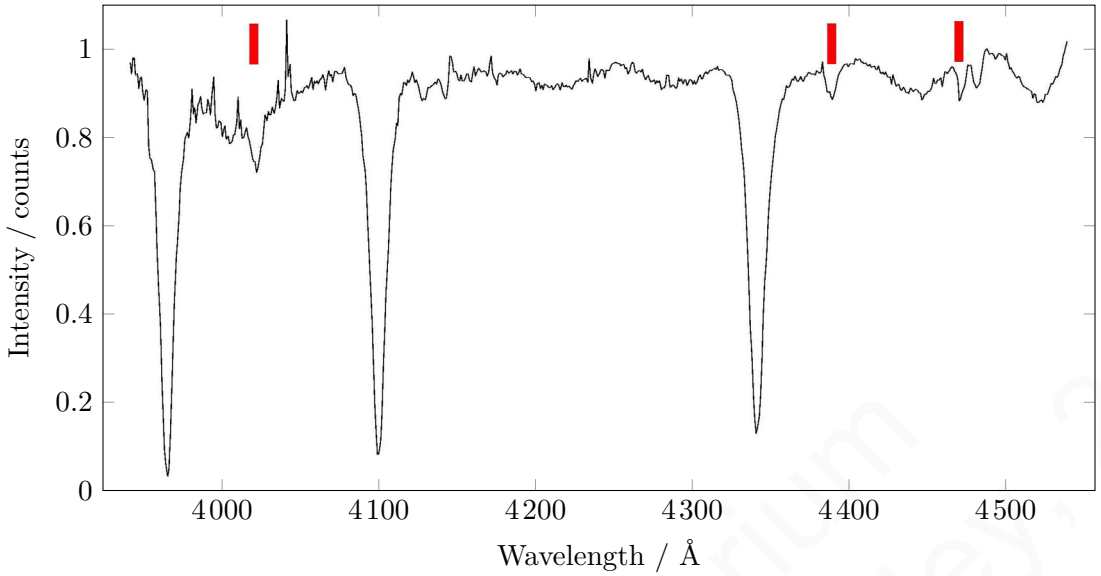

Figure 4.13: Spectrum of Regulus. The marks identify the He I lines used for the determination of the rotational velocity.

He I line	**Slope** m	**Offset** b	**See Fig. 4.14**
4026 Å	0.020	1.06	+
4388 Å	0.022	0.77	×
4471 Å	0.023	0.70	△

Table 4.7: Parameters, slope m and offset b, for the linear fits to the data representing the broadening of the helium lines due to intrinsic rotation of the star. From Daflon et al. (2007).

4.3.2 Error estimation

The error was calculated with standard error propagation. The widths of the He I lines are of the same order of magnitude as the width of the Hα line (in zero shift position), whose width was used for the determination of the binary system's mass in Section 4.2. The uncertainty in the measurements for the binary stars should be roughly the same as for the measurements of the He I lines. For that reason, the error on the measured width of the He I lines is $\Delta\mathrm{FWHM} = 0.685\,\text{Å}$, which is the average of the errors determined for AO Cassiopeiae (0.53 Å) and 44 Boötis (0.84 Å) in zero shift position. Because all measured linewidths are afflicted by the same error, the final error Δv_{rot} was determined to be:

$$\Delta v_{\mathrm{rot}} = \frac{\sqrt{3}}{3}\Delta\mathrm{FWHM} = 0.4\,\text{Å} \mathrel{\widehat{=}} 30\,\mathrm{km\,s^{-1}} \quad . \tag{4.5}$$

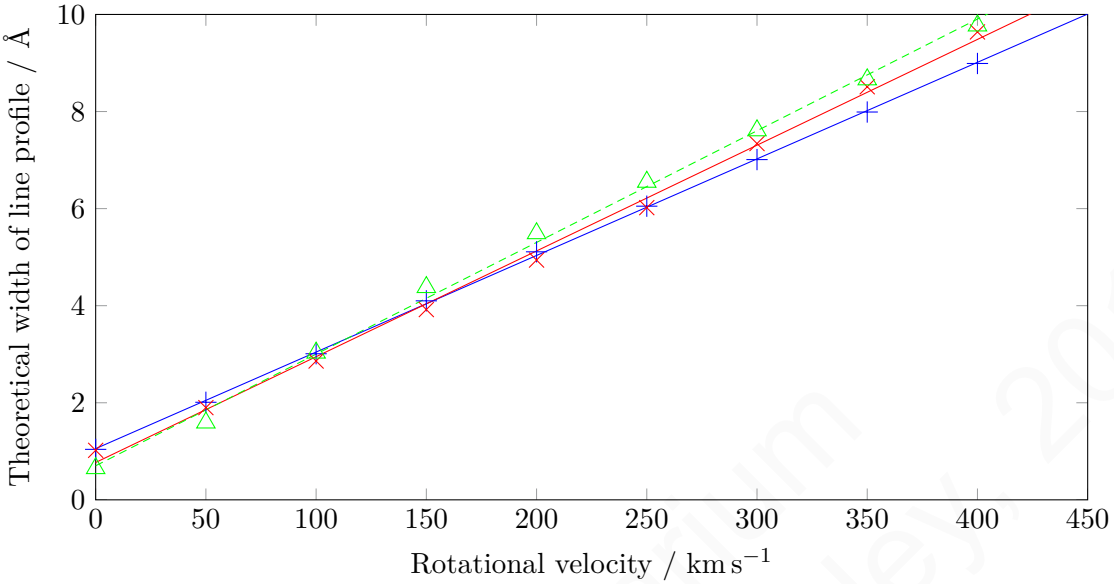

Figure 4.14: Theoretical linewidth vs. rotational velocity of a star with T_{eff} of 15 000 K for He I at 4026 Å (+), 4388 Å (×) and 4471 Å (△). For clarity the best linear fit is shown as a solid line. From Table 4.6a.

He I line	λ_1/Å	λ_2/Å	λ_3/Å
Measured FWHM	7.53 Å	7.61 Å	6.58 Å
After subtraction of instrumental line profile	7.34 Å	7.43 Å	6.36 Å
Resulting $v \sin i$	316 km s^{-1}	305.5 km s^{-1}	246 km s^{-1}

Table 4.8: Measured values for the full-width-half-maximum of the He I lines at wavelength $\lambda_1 = 4026$ Å, $\lambda_2 = 4388$ Å and $\lambda_3 = 4471$ Å of Regulus after having subtracted the instrumental line profile.

The determined rotational velocity of Regulus is 290 km s^{-1} ± 30 km s^{-1}.

4.3.3 Conclusions

SIMBAD lists Regulus with a rotational velocity of 300 km s^{-1}. The escape velocity of Regulus is approximately 700 km s^{-1}. Regulus was also examined by Slettebak et al. (1975) and, although they do not list the rotational velocity of Regulus, the average value measured by Slettebak et al. for the He I lines of Regulus is 6.12 Å so the value determined here (6.6 Å) is close to the one of Slettebak et al.. The helium lines are not very strong, although the signal-to-noise ratio of the exposure is 55. The result could be more accurate if the signal-to-noise ratio would be higher, so exposures with a longer exposure time are needed.

It was decided to fit the helium lines not from the continuum but the way the best fit was achieved.[4] All in all it can be said that by following this method the rotational velocity of a star can be reliably determined. The value in the literature[5] lies within the margin of error. For further determinations it is advisable to achieve a better signal-to-noise ratio because of the weakness of the He I lines.

4.4 Wind velocity of a Wolf-Rayet star

This chapter bases on Chapter 13 of de Boer & Seggewiss (2008). Wolf-Rayet (WR) stars are over $20\,M_\odot$ at birth and lose mass by strong stellar winds. The maximum wind velocities can be up to $3000\,km\,s^{-1}$ and mass loss rates lie in the range of 1×10^{-5} to 8×10^{-5} $M_\odot$/yr.
Depending on the elements which produce the strong emission lines in the wind, the spectral class of the Wolf-Rayet stars is subdivided into WR nitrogen (WN), WR carbon (WC) and WR oxygen (WO). Because the strong winds carry away the hydrogen envelope their stellar surface consists mainly of helium. In most cases no hydrogen emission lines are seen in their spectra. Wolf-Rayet stars are very hot, typically with effective temperatures higher than 50 000 K.
Wolf-Rayet stars with expanding envelopes develop a so called P-Cygni profile. To understand the formation of such a profile the geometry of the whole expanding shell needs to be considered. The P-Cygni profile is the sum of a strong emission line produced in the wind and the absorption spectrum that comes into existence because of the star being seen through the expanding envelope. See Fig. 4.15 from de Boer & Seggewiss (2008). The larger the wind velocity is, the further blue shifted is the blue edge of the absorption spectrum. Thus the maximal wind velocity can be derived using the blue edge of the absorption spectrum by measuring the distance between blue edge and center of the envelope emission (see $\Delta\lambda$ in the figure to the right in Fig. 4.15).

4.4.1 Measurement

WR 140 was chosen as an example for a Wolf-Rayet star because, with a magnitude of $V = 6.887\,mag$, it is brighter than most other Wolf-Rayet stars in the northern hemisphere. Figure 4.16 shows its spectrum in the wavelength range between 5400 Å and 6100 Å taken with the 900-line grating and an exposure time of 600 s. The higher peak belongs to the transition of C IV at 5801.33 Å.[6] All transitions are labeled in Fig. 4.16

[4] Normally the baseline of the fit lies in the continuum of the spectrum but because of a lot of noise and other lines in the direct neighborhood of the helium lines, the IRAF routines automatically tried to fit the collectivity of the neighboring lines. Thus to determine the width of only the He I line, the baseline was shifted, in y-direction, so that only the He I line was fitted.

[5] `http://simbad.u-strasbg.fr/simbad/`, accessed on August 29., 2011.

[6] From `http://www.nist.gov/pml/data/asd.cfm`, accessed on August 29., 2011.

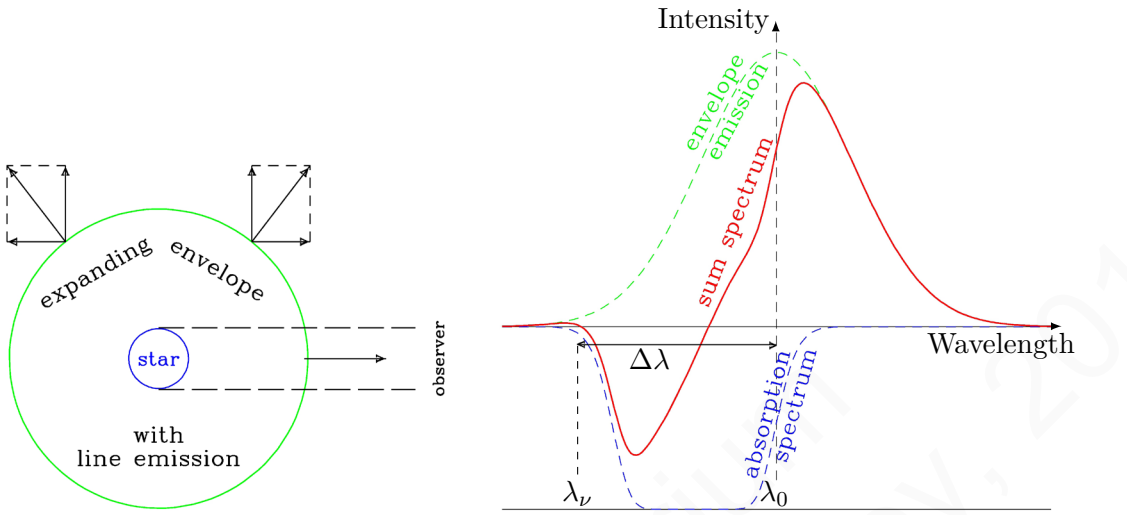

Figure 4.15: Sketch of the geometry of a WR star wind (left) and the resulting P-Cygni profile of a wind-emission line with absorption through the expanding envelope. Figure from de Boer & Seggewiss (2008).

and as a reference for the identification was used Fig. 5 from Marchenko et al. (2003). The blue edge at 5737 Å was measured with the IRAF task *splot*. The measured difference ($\Delta\lambda$) between the center (λ_0) of the C IV (5801.33 Å) line and the blue edge ($lambda_\nu$) was 64 Å. Thus with Equation (3.1) this leads to:

The stellar wind velocity of WR 140 was $3300\,\mathrm{km\,s^{-1}} \pm 400\,\mathrm{km\,s^{-1}}$

4.4.2 Error estimation

Determining the uncertainty in the measurements made here was not easy due to poor statistics: only one spectrum was available. The resolution of the spectrograph was (in this wavelength range) approximately 3000. The intrinsic error was roughly $100\,\mathrm{km\,s^{-1}}$. The blue edge was rather flattened and the determination of its exact position was afflicted with an uncertainty. Thus the total uncertainty on the wind velocity was estimated to be $\pm 400\,\mathrm{km\,s^{-1}}$.

4.4.3 Conclusions

The result is consistent with the published value given in de Boer & Seggewiss (2008) for the maximum wind velocity. The magnitude of the wind velocity is surely larger than

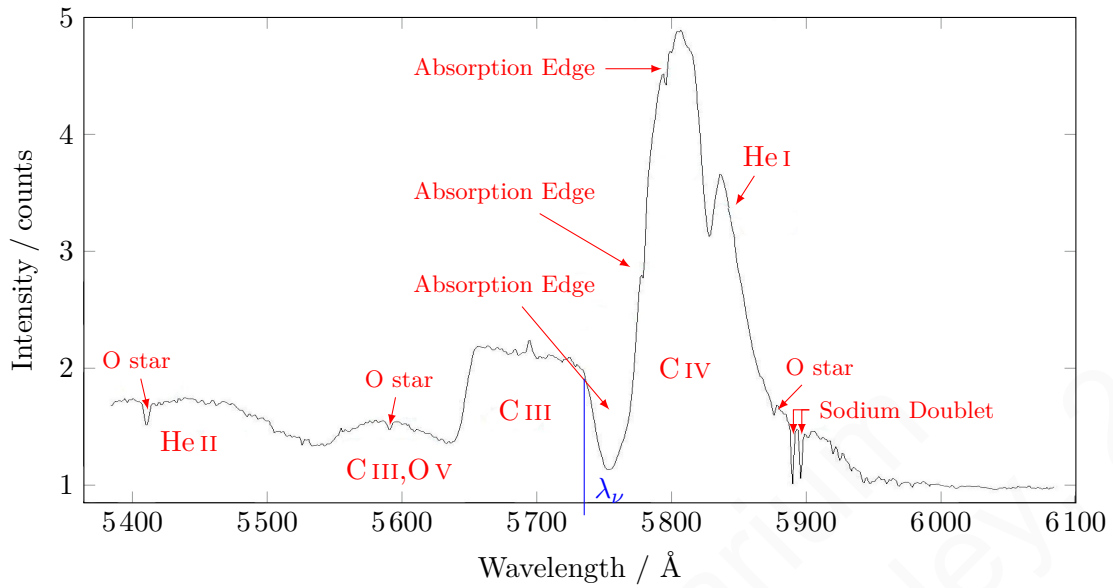

Figure 4.16: Here is shown a part of the spectrum of WR 140 taken with the 900-line grating and an exposure time of 600 s. WR 140 is a WC7 type star, that means it shows strong emission lines of Carbon. Furthermore it is a bright object ($V = 6.88$ mag), that can be observed with moderate exposure times with the AIfA-telescope. WR 140 is actually a binary star, that is why there are also oxygen absorption lines in the spectrum. λ_ν represents the maximum blue shifted part of the absorption spectrum and thus the maximum wind velocity.

the escape velocity of the Wolf-Rayet star (which lies around 1500 km s^{-1}). Thus it is understandable that Wolf-Rayet stars have such big mass loss rates.

Chapter 5

Conclusions & Outlook

5.1 Summary

The achievement of this diploma thesis is a reasonable and interesting bachelor laboratory course which uses the 50 cm-Cassegrain-telescope of the *Argelander Institut für Astronomie*. The course enriches the repertory of already existing laboratory courses at the Physikalische Institut and gives the *Argelander Institut für Astronomie* the opportunity to let Bachelor students experience astronomical work. In the following there will be given a short summary of the thesis.

- Chapter 2 explains the instrumental set-up as well as a description of detailed examinations of the components, such as the resolution of the spectrograph, the determination of the best focus of the spectrograph, the determination of gain and readnoise as well as the signal-to-noise ratio as a function of a stars magnitude and the exposure time. The resolution was best around 6500 Å namely $R = 3300$ (for the 900-line grating), thus it was decided to use the Hα line at 6562.8 Å for the measurements. The position of the best focus of the spectrograph was earmarked on the spectrograph so that a reference point was given for the vernier adjustment that needs to be done before each measurement. The results of the measurement of gain K and readnoise N_R are:

  - Gain $K = 1.5$ electrons/count
  - Readnoise $M = 17.8$ electrons/pixel

  It was consciously decided not to do an error calculation because these values are just for the orientation.
  Table 2.5 lists the signal-to-noise ratio as a function of a stars magnitude and the exposure time.

- Chapter 3 summarizes the physics background about line broadening mechanisms needed for the completion of the laboratory course.

- In Chapter 4 the measurements and the results are presented. Two binary star systems were observed (44 Boötis and AO Cassiopeiae) to determine their total

mass, Regulus, as an example of a fast rotating star, to determine its rotational velocity and WR 140 to determine the velocity of its stellar wind by using the broad emission lines of the spectrum. The results are:

  - Mass of 44 Boötis: $1\mathrm{M}_\odot \pm 0.3\mathrm{M}_\odot$
  - Mass of AO Cassiopeiae: $24\mathrm{M}_\odot \pm 1.5\mathrm{M}_\odot$
  - Rotational Velocity of Regulus: $290\,\mathrm{km\,s^{-1}} \pm 30\,\mathrm{km\,s^{-1}}$
  - Wind velocity of WR 140: $3300\,\mathrm{km\,s^{-1}} \pm 400\,\mathrm{km\,s^{-1}}$

- In the Appendix all required documentation can be found that will be handed out to the students and is needed for the completion of the laboratory course.

All results are in good agreement with published values. Thus, it can be said that the methods used are reliable. Already three groups of students accomplished the course successfully in early summer 2011. The students gave positive feedback and agreed that the tasks were appropriate for third year Bachelor students.

5.2 Outlook

In spite of the level of work focused on all aspects of the laboratory course, there are still some open questions and some issues that should be addressed.

- Because of the high orbital velocities of AO Cassiopeiae, the resolution of the spectrograph is sufficient enough that -at maximum shift position- the stellar spectral lines can almost be individually resolved. IRAF provides a deblending task that fits two Gaussian functions in spectral lines, instead of one. Thus, the total shift between the two spectral lines would be the difference between the two fitted centers of the Gaussian functions. It would be interesting to consider whether this method leads to the same results for the masses of the binary systems as the one discussed in this work.

- The dataset for AO Cassiopeiae is rather scarce, so more data is needed. One idea is for the students to observe more binary systems, with longer periods, but always the same systems, in order to obtain more data and to finally have larger data sets for different binary systems. By adding one data point to the set but evaluating the whole set, the laboratory course would be the same but, over time, there would be a larger sample of binary stars for students to choose from.

- In general more data is needed to yield better statistics and more reliable results.

The weather is unpredictable, thus more archived data is needed for students who may not have the chance to observe themselves.

- Binary stars, Wolf-Rayet stars and fast rotating stars are not the only objects that can be observed. The laboratory course could be expanded significantly to include other interesting astrophysical systems. For example it would be an interesting question if it is possible to measure the expansion of the Crab nebula.

The laboratory course will be offered twice a year. Within each cycle improvements will be made, and new and interesting exercises may be added to the core laboratory material.

Appendix A

Test record

A.1 Intention of the laboratory course

During this laboratory course stellar spectra are observed to determine various parameters of stellar systems: the total mass of a binary star system; the rotational velocity of a star; and the wind velocity of a Wolf-Rayet star. The Doppler effect and its consequences for observed stellar spectra is a central point. The students will expand their knowledge of atomic structure, they will observe self-governed with the AIfA 50 cm-telescope (including DADOS spectrograph and ST 402 ME camera) and reduce and evaluate data with modern data reduction software.

A.2 Prerequisites

1. What is spectroscopy?
2. Atomic structure
3. Line broadening mechanism
4. Stellar classification (spectral classes)
5. Wolf-Rayet stars
6. Kinematics of binary star systems, radial velocity curve
7. The Doppler effect
8. Diffraction Grating/Functionality of a spectrograph

9. Functionality of a CCD (briefly)
10. Spectroscopic fringes
11. Telescopes, telescope mounts, AIfA-telescope

12. Data reduction of astronomical CCD data (Flat, Bias, Dark)
13. Modified Julian Date (MJD)

A.3 Literature

1. H. Haken & H. C. Wolf - Atomic and Quantum Physics, Springer, 2004
2. K. S. de Boer & W. Seggewiss - Stars and Stellar Evolution, EDP Sciences, 2008
3. A. Unsöld - The new cosmos, Springer, 2005
4. S. B. Howell - Handbook of CCD Astronomy, Cambridge University Press, 2000
5. C. R. Kitchin - Optical astronomical spectroscopy, Taylor & Francis Group, 1995
6. A User's Guide to reducing slit spectra with IRAF (`http://iraf.noao.edu/docs/spectra.html`, accessed on September 6., 2011.)
7. W. D. Heintz - Doppelsterne, Goldmann, 1971
8. J. Martin - A spectroscopic Atlas of Bright Stars, Springer, 2010

A.4 Tasks

1. Carry out a measurement where the whole spectrum of the calibration lamp will be recorded to get an overview of its spectrum.[1]
2. Determine the dispersion for all frames of the calibration lamp (during daytime).
3. During the night, object frames and calibration frames/flats are taken after having

[1] Check out the focus setting. Can it be improved? Use CCD SOFT for a vernier adjustment of the focus.

carefully decided which objects to observe, at what time exactly. Take data of:

- A binary star system
- A fast rotating star
- A Wolf-Rayet star

4. Reduce the data with IRAF[2].

5. Determine the resolution of the spectrograph in the wavelength range you want to observe. Is the resolution good enough to be able to measure the broadening of a stellar spectral line of the desired object? Assume that the DADOS has a resolution of R=3000. How fast must be the rotation of a star that it can be measured with the given set-up? Give an estimate of how big the orbital velocity of a binary system has to be, to be measurable.

A.5 Experimental Procedure

- BEFORE you start observing make a plan of which object you want to observe at what time during the night. Stars rise and sink at the sky and most of them are not visible during the whole night. Furthermore the chosen binary system shall be observed at times when the spectral lines show no shift and when they show maximum separation (Doppler effect). These points in time can be calculated. Keep in mind: Observing time is precious and the search for suitable objects takes time.

- Calibration frames HAVE TO be taken DIRECTLY after the respective object frame BEFORE moving the telescope. Flat field exposures should be taken before the grating is tilted but if the wavelength calibration is done accurately it can also be taken at the end of a night.

- It is advisable to start an observing protocol, in which will be marked object number, name of object, exposure time, camera temperature, value of micrometer screw, notes etc...

- The camera is controlled with CCD Soft. In case questions come up, the manual can be found online.[3]

- The time written in the header of the taken images is the computer time. It can

[2] Image Reduction and Analysis Facility.

[3] `http://www.bisque.com/help/ccdsoft\%20info/ccdsoft_version_5_user_s_manual.htm`, accessed on September 5., 2011.

be synchronized via Internet (right click on the clock symbol, "Datum/Uhrzeit "ändern", "Internetzeit", "Einstellungen "ändern" → "jetzt synchronisieren").

- The stellar spectra need to be wavelength calibrated. To be able to identify the calibration lines, an overview measurement needs to be done. Take images of the calibration lamp at 0 µm, 35 µm, 70 µm ... (**Loosen the grating before tilting it!!!**, just turn the screw in one direction to avoid backlash). Identify the calibration lines with help of the printed spectra in Appendix A.7 and find out the relation between value of the micrometer screw and the displayed wavelength range. This measurement will approximately take two hours of time (the data will be reduced with IRAF). Start early enough so you do not lose observing time.

- Determine the dispersion of the images and the wavelength dependent resolution of the spectrograph.

- Start observing the chosen objects. The following list includes some suitable objects (**Question:** Why are these objects suitable and what for?).

  Unfortunately the read out of the camera is not working well and an echo of the just taken image stays on the chip and will be overlaid with the next taken image. To get rid of this echo, the CCD chip needs to be read out several times until no echo is left (approximately five darks of one minute exposure time).

  1. AO Cassiopeiae
  2. 44 Boötis
  3. Regulus
  4. WR 140

  You can chose other objects. A catalog including many binary systems can be found online (Batten et al. 1989). In this catalog are also listed the information of period, mass, orbital velocity etc. For more information see Appendix A.7. The signal-to-noise ratio of the spectra has to be better than 35. (**Question:** What is a signal-to-noise ratio? How can it be calculated?)

- No flux calibration is needed since the Doppler effect has an impact on the widths of the spectral lines, not on the intensity.

- A useful flat field should have a high signal-to-noise ratio. Take 10 minutes exposure time for a flat field. The illumination should be higher than 20 000 counts. If this is not the case, take another flat field of 10 min exposure time and stack the two afterwards.

- At the end copy the taken data to an USB stick.
- Reduce the data with IRAF. The IRAF manual is given in the appendix. Document your proceedings in the *laboratory report*. All taken spectra need to be displayed including the fits to the spectral lines.

1. Reduce the data regarding flat, dark, bias...
2. Do a wavelength calibration, identify the stellar lines, verify the spectral type of the star.
3. Determine the mass of a binary star system.
4. Determine the rotational velocity of a fast rotating star, compare it to its escape velocity.
5. Determine the wind velocity and temperature of a Wolf-Rayet star.

A.6 Test record and set-up

The telescope and spectrograph manual can be found in the dome or online.[4] The suitcase with the spectrograph is in the cupboard in the anteroom of the dome. Please be careful when handling the spectrograph and do not touch any optical surfaces. Ask the tutor to show you how to mount the spectrograph to the telescope.

If it starts raining, IMMEDIATELY put the telescope cover over the primary mirror and close the dome, tell the tutor.

A.7 Appendix

1. IRAF Manual
2. Table of exposure times
3. Parameters of the SBIG ST 402 ME
4. Spectrum of the Calibration Lamp
5. Explanation of "Spectroscopic binary catalog"

[4] `http://www.astro.uni-bonn.de/~astroclub/AIfA_telescope_manual.pdf`, accessed on September 25., 2011

(Some of the appendices can only be obtained from the tutor).

Appendix B

IRAF Manual

B.1 General Information

1. IRAF is the acronym for *Image Reduction and Analysis Facility.* The reduction process was based on the "User's Guide to Reducing Slit Spectra with IRAF" by P. Massey, F. Valdes and J. Barnes.[1] IRAF is an old but very valuable image reduction program. It is segmented into packages and tasks. To have access to a specific task it is necessary to change into the package including the wanted task. Type `help taskname` into the IRAF terminal and the package including the task will be displayed as well as an elaborated help page.

   To start IRAF, type (into the LINUX terminal from the directory where IRAF is located):

   - cd iraf
   - iraf . -9

2. You have to edit parameters. Every task has it's own parameter set which can be modified and thus adapted to the data. Type `epar taskname` to edit the parameters. To save changes type `:wq` in the "edit parameter" menu. If you want to leave the menu without saving, type `:q`. (`:w` writes the changes into the "uparm" directory ("user parameter" directory)). To reset the parameters of a specific task type `unlearn taskname`.

3. After having executed specific tasks on the images, IRAF will ask under which name to save the changes. Please stick to the following convention:

   a) Starting image: obj001.fit

   b) After dark subtraction → obj001m.fits

   c) After task `dispcor` → dobj001m.ms.fits

[1] `http://iraf.noao.edu/docs/spectra.html`, accessed on September 6., 2011.

d) After dividing by the flat field →fdobj001m.ms.fits

e) After task `continuum` → kfdobj001m.ms.fits

WATCH OUT: No periods "." in the image names e.g. do not name an image obj001.m.fits, name it obj001m.fits because IRAF can't read periods. IRAF will name an image after having extracted it `obj001m.ms.fits`. In this case `.ms` stands for "multispec" format and thus for a format change, not for a name change.

B.2 Image reduction in respect of darks and flats

Darks have to be subtracted before the spectrum will be extracted. Unfortunately it happens that cosmic rays or echoes of the calibration lamp appear in dark exposures. For this reason you should take at least three dark frames and combine them with the task *imcombine* to get a masterdark. *Imcombine* does not belong to a specific package and can be used no matter what package is invoked. To get rid of cosmic rays, set the parameter `reject` on `crreject` (type `epar imcombine` and read through the parameters to find `reject`). The input images for *imcombine* must either be written in a wildcard or in a list:

```
ls *.fit > listname.dat
```

If a list is used then the input (in `epar imcombine`) must be `@listname.dat`. The division by the flat field exposures will be done after the wavelength calibration - see Section B.5.

B.3 Extraction of spectrum

The raw images you get out are two-dimensional images which show just the image of CCD chip. Figures B.1 and B.2 show two examples of stellar spectra taken with the DADOS spectrograph after dark subtraction. Figure B.1 shows a spectrum of Regulus ($V = 0.03$ mag with an exposure time of 120 s) with a signal-to-noise ratio of more than 50. Figure B.2 shows a spectrum of AO Cassiopeiae ($V = 6.102$ mag; exposure time: 600 s) with a worse signal-to-noise ratio but still more than 35. The signal-to-noise ratio was determined in the continuum spectrum. The detailed method how to determine the signal-to-noise ratio is described in Section B.9.

The spectrum of Regulus is thinner, which is due to better focusing. To obtain usable data the signal-to-noise ratio should not be worse than 35. See Table B.1 for more details on exposure times and associated signal-to-noise ratios.

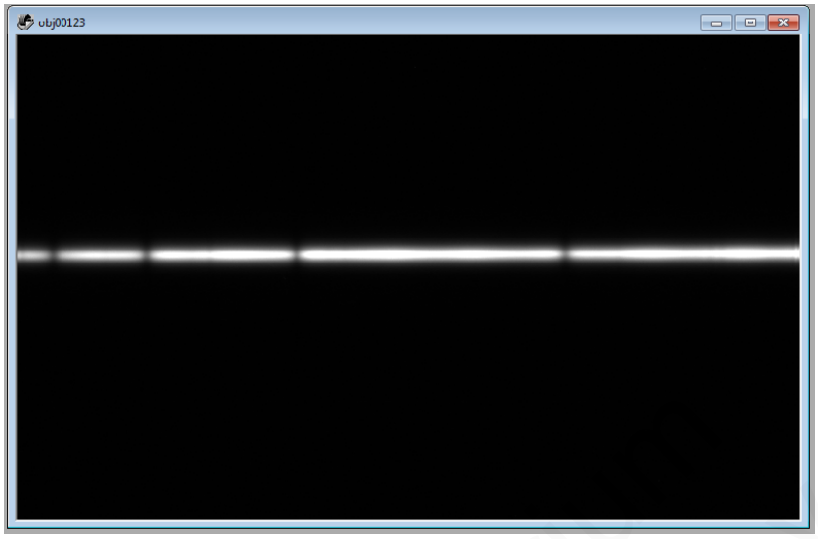

Figure B.1: Example of a spectrum of Regulus with good signal-to-noise ratio. This spectrum was taken with the 900-line grating and an exposure time of 120 s. The brightness (in the visual part of the spectrum) of Regulus is $V = 0.03$ mag (from `http://simbad.u-strasbg.fr/simbad/`, accessed on August 29., 2011). With help of the slit viewer, the star is centered on the middle (smallest) slit. The contrast was adjusted in a way that only the image of the star (spectrum) is seen and the rest of the image appears black.

To extract the spectrum use the package *apextract* with the task *apall* (noao → twodspec → apextract → apall). Check if the dispersion axis lies along lines or along columns. To do so go to `epar apextract`.

- `epar apextract`
- `dispaxi = 1 or 2`

Now check in what range of the CCD the spectrum lies, because IRAF will search for it automatically on the CCD in this given area. It is assumed the spectrum lies along lines, use the task *implot* to find out where it lies. *Implot* starts with the command `implot imagename`. Another window ("irafterm") opens. To prevent an IRAF crash do not close the irafterm window with "`x`". Always leave it by typing "`q`" in the activated window. It happens that the image just shows background noise (see Fig. B.3). The reason for that is that the default setting of *implot* plots the middle line, thus line 255 (the CCD has approximately 500 lines and 700 columns). The spectrum crosses column 1 and column 700 at different lines. `:l 197` or `:c 300` are examples to plot line 197 or column 300. With *implot* it can thus be found out where on the CCD the spectrum lies. Figure B.4 shows a plot of column 10. The commands ":c 10" etc are typed into the irafterm window where the plot is displayed, not in the IRAF terminal. If it happens

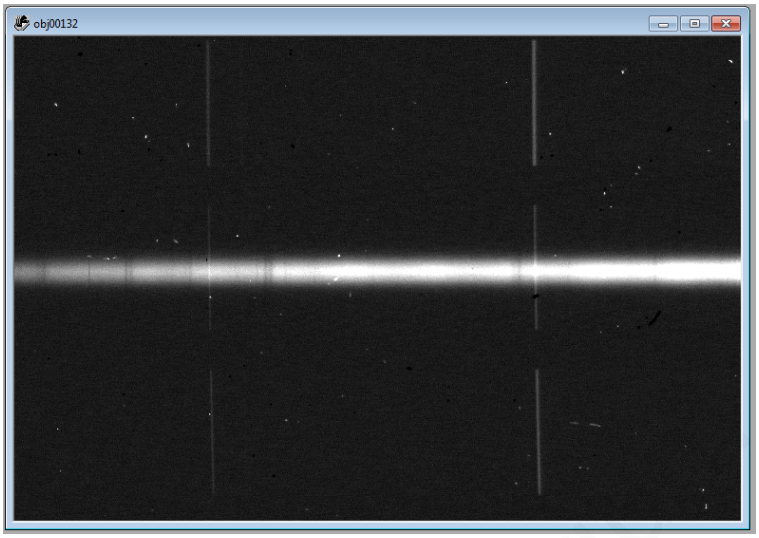

Figure B.2: Example of a star with worse signal-to-noise ratio than the one of Fig. B.1, overlaid by the echo image of the calibration lamp. This spectrum of AO Cassiopeiae used an exposure time of 600 s and was also taken with the 900-line grating. The brightness (in the visual part of the spectrum) of AO Cassiopeiae is $V = 6.102$ mag (from `http://simbad.u-strasbg.fr/simbad/`, accessed on August 29., 2011). With help of the slit viewer, the star was centered on the middle (smallest) slit. The contrast was adjusted in a way that only the image of the star (spectrum) is seen and the rest of the image appears black.

that it is not possible to say where the spectrum lies and to distinguish between signal and noise, then the signal-to-noise ratio is not good enough and you should get exposures with a better signal-to-noise ratio (longer exposure times). Type capital "`C`" to see at which line the spectrum starts and where it ends. Two numbers are displayed on the bottom left of the irafterm window, the left number is the pixel number, the right one is the pixel value at that point. Determine where the peak starts and where it ends and note the values. IRAF needs this information later on to have a starting point to search for the spectrum and a reference for at what point lies the maximum from where on the spectrum extends up and down. It is possible to stick to "nice numbers" e.g. 45 instead of 43. EXAMPLE: At column 10 the spectrum goes from line 187-262 and at column 690 from line 190-262. The middle is at approximately 255 and the spectrum extends not further than 35 pixels up and down from the middle line. To be sure that the spectrum lies inside this range of 35 pixels, it is advisable to set the range to ±40pixels. The same procedure is done to find out where the background begins (a pixel value further away than 40 pixels from the middle 255). This area lies between the red and green marks in Fig. B.4. The area in between the red marks represents the spectrum.

Now start with the task *apall*. *Apall* has to be edited to put in the just gained information

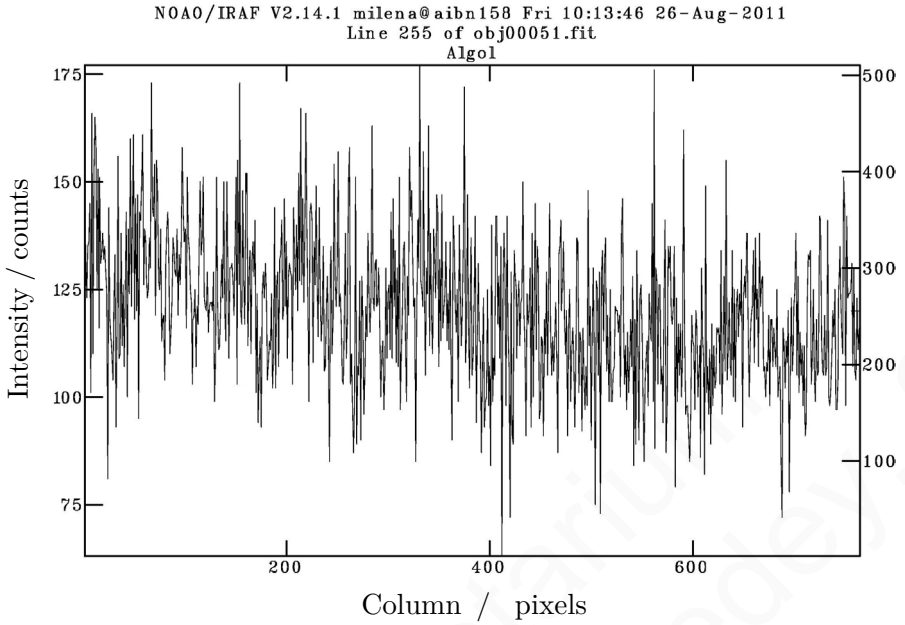

Figure B.3: Implot of line 255. The image just shows background noise.

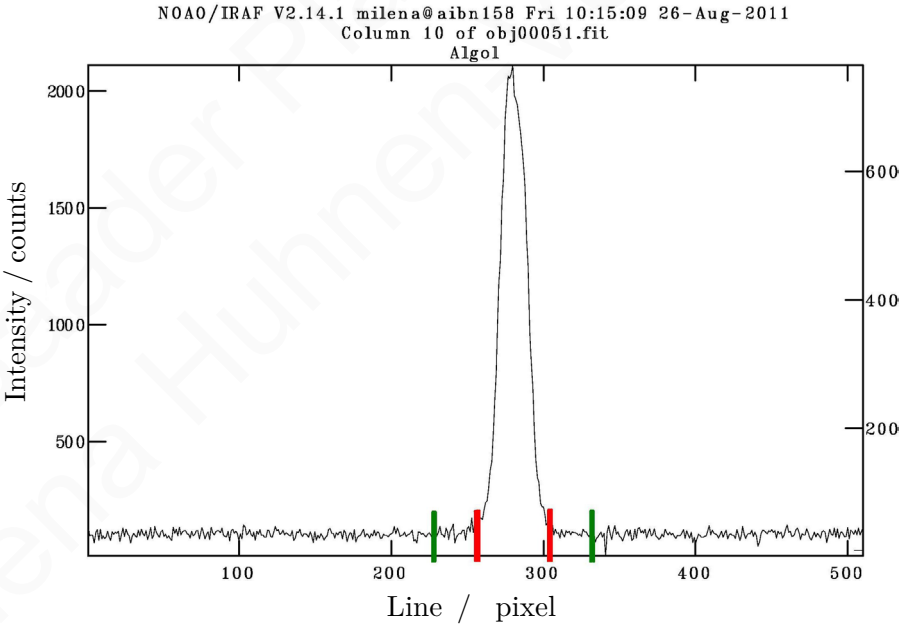

Figure B.4: Implot of column 10. The background lies in between the two marks on each side of the spectrum. The area in between the inner marks includes the spectrum.

of the location of the spectrum. Thus type `epar apall` into the IRAF terminal and set the parameters to the following values. It is important that you compare and set the parameters in your IRAF session to the parameters given here.

Parameter	**Value**	**Remark**
apertur		
format	multispec	
referen		
profile		
interac	yes	
find	yes	
recente	yes	
resize	no	
edit	yes	
trace	yes	
fittrac	yes	
extract	yes	
extras	yes	
review	yes	
line	INDEF	IRAF searches the area of the CCD that was determined with *implot* and uses the intensity to decide whether or not it is spectrum or background. Leave this parameter on INDEF.
nsum	100	

Default Aperture Parameters		
Parameter	**Value**	**Remark**
lower	···	Here type in the value, determined with *implot*, how far from the middle the spectrum goes down (in our case -40).
upper	···	Here type in the value, determined with *implot*, how far from the middle the spectrum goes up (in our case +40).
apidtab		

Default Background Parameters		
Parameter	**Value**	**Remark**
b_funct	chebyshev	
b_order	1	
b_sampl	...	Here type in the values determined with *implot* to deduct the background from the spectrum. Leave enough space between the point where the spectrum ends and where the background begins, to be sure that there is no intensity from spectrum in the background area. EXAMPLE: If the spectrum ends at ±40, start the background at ±55 and take 10 to 20 lines into account. Type in `-70:-55,55:70`.
b_naver	100	
b_niter	0	
b_low_	3.	
b_high	3.	
b_grow	0.	

Aperture Centering Parameters		
Parameter	**Value**	**Remark**
width	...	Type in the maximum width of the spectrum determined with *implot*. For the given example that would be 80.
Radius	10.	
thresho	0	

Automatic Finding and Ordering Parameters		
Parameter	**Value**	**Remark**
nfind	1	
minsep	5.	
maxsep	1000.	
order	increasing	

Recentering Parameters		
Parameter	**Value**	**Remark**
aprecen		
npeaks	INDEF	
shift	yes	

Resizing Parameters		
Parameter	**Value**	**Remark**
llimit	INDEF	
ulimit	INDEF	
ylevel	0.1	
peak	yes	
bkg	yes	
r_grow	0	
avglimi	no	

Tracing Parameters		
Parameter	**Value**	**Remark**
t_nsum	10	
t_step	10	
t_nlost	3	
t_funct	legendre	
t_order	2	
t_sampl	*	
t_naver	1	
t_niter	0	
t_low_r	3.	
t_high_	3.	
t_grow	0.	

Extraction Parameters		
Parameter	**Value**	**Remark**
backgro	fit	
Skybox	1	
weights	none	
pfit	fit1d	
clean	no	
Saturation	65536.	
readnoise	17.8	
gain	1.5	
lsigma	4.	
usigma	4.	
nsubaps	1	
mode	ql	

All changes have to be saved into the user parameter directory (with ":wq"). Start *apall* by typing `apall` into the IRAF terminal.

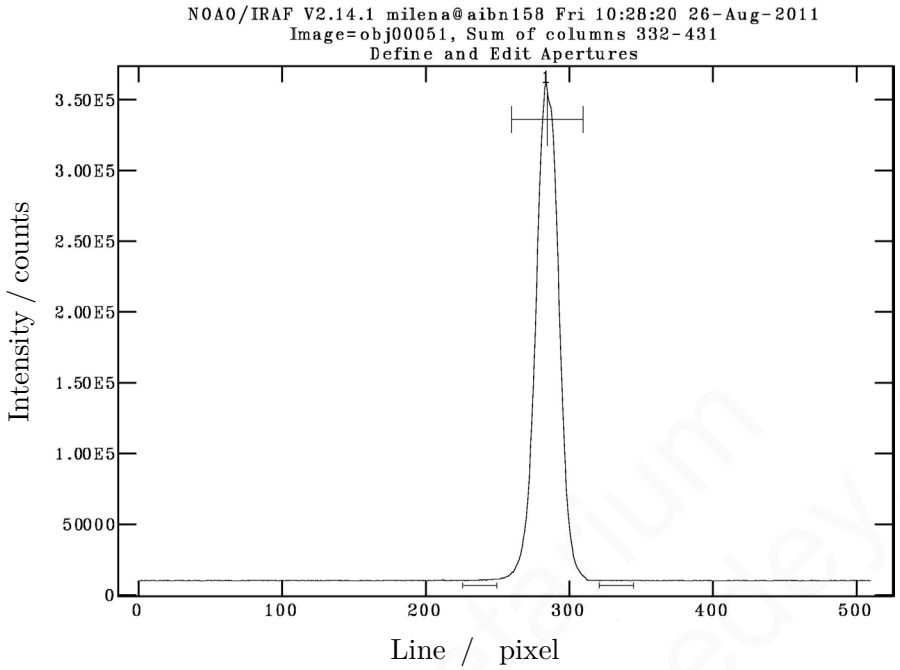

Figure B.5: Aperture Editor.

```
List of input images - imagename
Find apertures for imagename - yes
Number of apertures to be found automatically - 1
Edit apertures for imagename?  - yes
```

Now you are in the aperture editor where it is possible to reset the parameters typed into *apall* in case you notice that the chosen apertures were badly chosen. You can see the apertures in the new irafterm window. They look like errorbars (see Fig. B.5). Press "`?`" (in the irafterm window) to get a list with all cursor commands. "`l`" sets the lower aperture limit to cursor position, "`u`" sets the higher aperture limit to cursor position. "`d`" deletes apertures. By pressing "`b`" the background editor will open where badly chosen background apertures can be deleted with "`z`" and reset with "`s`". "`q`" brings you back to the aperture editor and if you type again "`q`" you will leave the aperture editor to come to the trace editor. For more information read the script "Reducing Slit Spectra with IRAF". In the trace editor the following questions have to be answered:

```
Trace apertures for imagename?  - yes
Fit traced positions for imagename interactively?  - yes
Fit curve to imagename interactively?  - yes
```

Now you can see the fit to the "trace", e.g. the run of the spectrum on the CCD. The fitting order can be increased in case the fit deviates too far from the data points (for

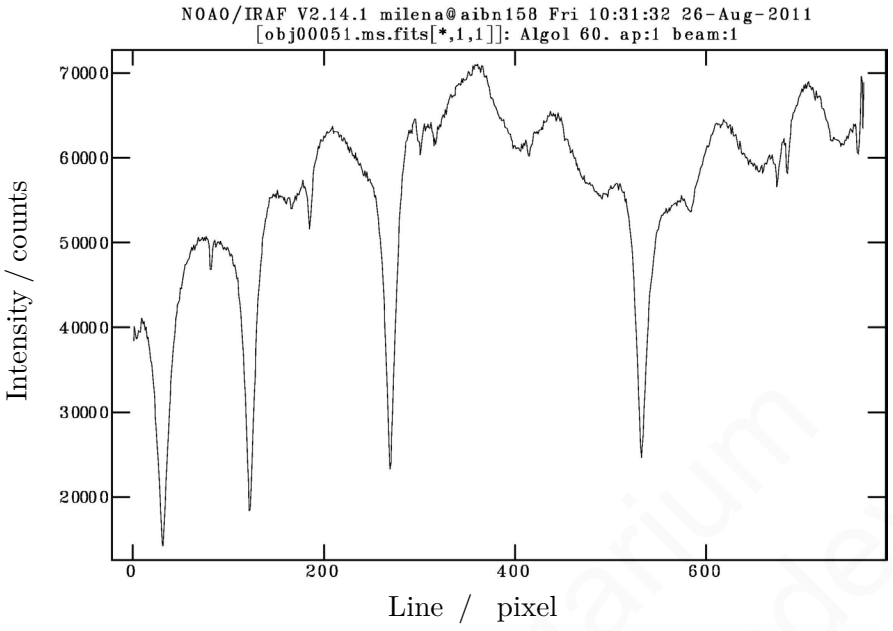

Figure B.6: An extracted spectrum of Algol. Note the spectroscopic fringes, this spectrum is not yet flat field corrected. See Section B.5 to learn how to remove the fringes.

order 3 type `:order 3` in the irafterm window). The cursor commands in this fitting routine are different from the aperture or background editor. Just type ":" and the name of the parameter to be changed e.g. `:order`. Data points can be deleted with "`d`". Press "`f`" for a new fit. If the fit to the trace satisfies the demand, press "`q`".

```
Write apertures for imagename to database?  - yes
```

"Database" is a "directory" which is created automatically by IRAF and where data is saved such as the apertures of the extraction parameters etc. In case it is necessary this information can be deleted.

```
Extract aperture spectra for imagename?  - yes
Review extracted spectra from imagename?  - yes
Clobber existing output image imagename.ms ?  - yes oder no...
Review extracted spectrum for aperture 1 from imagename?  - yes
```

Figure B.6 shows the extracted spectrum. IRAF names the images of the extracted spectra `imagename.ms.fits`. .ms stands for the multispec format. At the extracted spectra can be looked with the task *splot* (noao → onedspec → splot). Sometimes it occurs that although a dark subtraction was made that there is still a hot pixel in the spectrum (see Fig. B.7). The "spectral line" caused by the hot pixel can be deleted (in

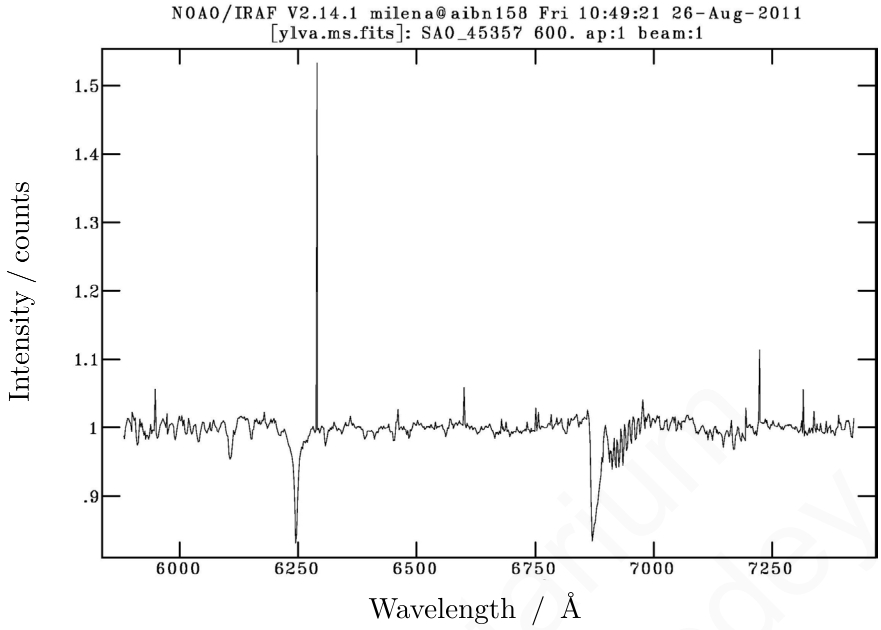

Figure B.7: Spectrum of 44 Boötis with a hot pixel at ca 6290 Å.

the irafterm window when the image is viewed with *splot*) with the cursor command `"j"`. `"j"` fudges a point to y-cursor value. Use cursor command `"i"` to save the changed image.

B.4 Wavelength calibration

After the spectrum is extracted a wavelength calibration is needed, which is done by mapping pixels to wavelengths. The spectrum of the calibration lamp has to be extracted the same way as the one of the object frame. IRAF wrote the extraction parameters of the object frames in the headers of these frames. With the following command IRAF reads these extraction parameters and uses them for the extraction of the calibration image belonging to the respective object frame:

```
apall laser00001 out=claser00001 ref=obj00001m recen- trace- back- intera-
```

In this case the original image is called `obj00001.fit` and the corresponding calibration frame `laser00001.fit`.

```
Searching aperture database ...
Date, Time:  DATABASE - 1 apertures read for obj00001 from database
Date, Time:  DATABASE - 1 apertures for laser00001 written to database
```

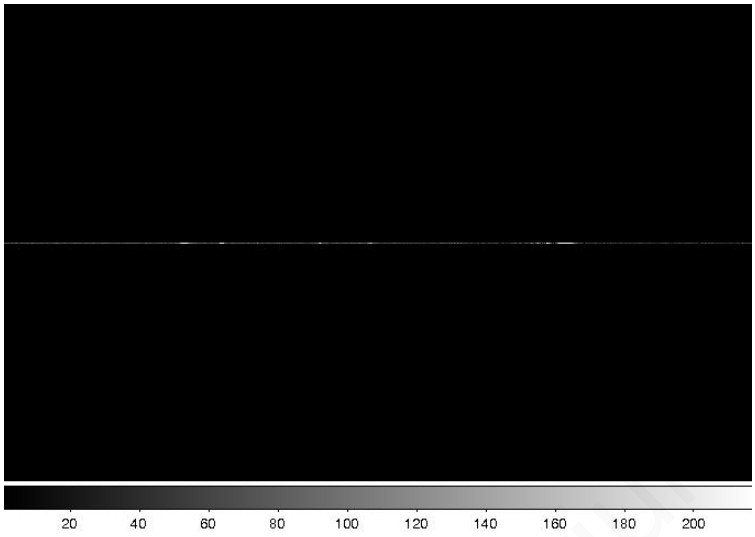

Figure B.8: Extracted, one dimensional calibration spectrum.

```
Extracting apertures ...
Date, Time:  EXTRACT - Aperture 1 from laser00001 → claser00001
```

Image frame and calibration frame have to be in the same folder! Make copies of your images! Calibration frames that were extracted are called with a "c" in front: laser001.fit → claser001.fits. The extracted calibration frame is one dimensional. Look at it with by typing `display claser00004.fits` (Fig. B.8). The spectral lines in the calibration frame have to be identified. Use *identify* (noao → onedspec → identify).

```
identify
Images containing features to be identified:  claser00001.fits
```

Again the irafterm window will open and shows the spectral lines of the calibration lamp. On the basis of the spectra given to you by the tutor you should be able to identify the spectral lines. With the cursor go over an identified line and press "`m`". If IRAF does not recognize the line, check the parameter `fwidth` in `epar identify`. Set this parameter to 4. If two lines are identified press "`l`" so IRAF identifies all other lines. If you made a mistake the identified values of the lines can be deleted with "`d`". IMPORTANT: After having identified all lines you have to press "`f`" to start the fit for the mapping between pixels and wavelength.

```
Write feature data to the database?  - yes
```

The identified calibration spectrum now has to be connected to the object frame. To do so write its name into the object frames header so IRAF will use it for the dispersion correction.

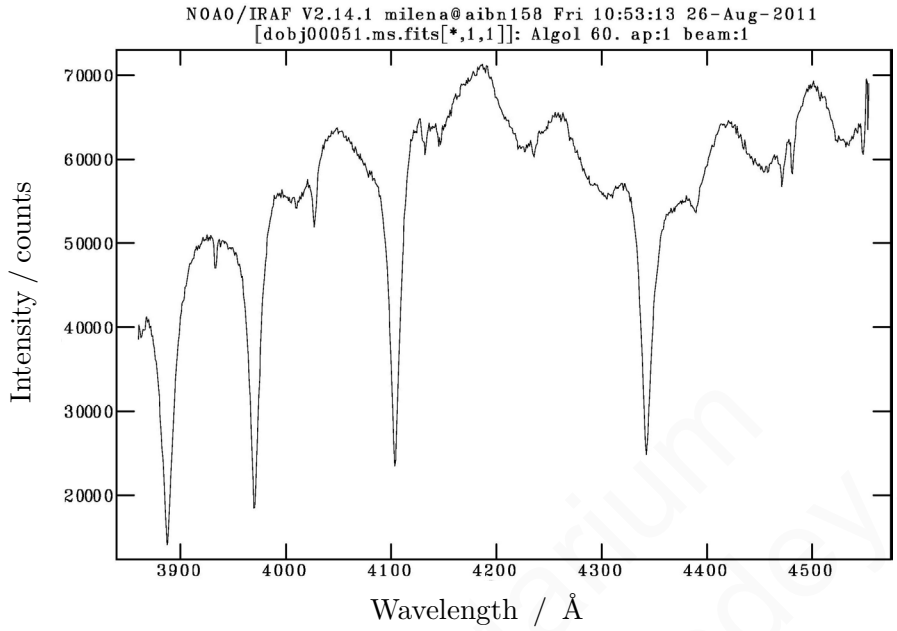

Figure B.9: Spectrum of Algol with wavelength scale. This spectrum is not divided by a flat field. The spectroscopic fringes are still visible.

```
hedit obj00001m.ms.fits REFSPEC1 "claser00001.fits" add+ ver- show+
add obj00001, REFSPEC1 = claser00001
obj00001.ms.fits updatet
```

Finally the dispersion correction has to be done. Type `dispcor` into the iraf terminal.

```
List of input spectra:  (obj00001):  - obj00001.ms.fits
List of output spectra (dobj00001):  - dobj00001.ms.fits
```

Dispersion corrected images are called with a "d" in front.

```
obj00001.ms.fits:  REFSPEC1 = 'cneon00004.fits 1.'
dobj00001.ms.fits:  ap = 1, w1=5732 w2 = 7222, dw = 1,95, nw = 765
```

Use *splot* to see the result (Fig. B.9).

```
splot dobj00001m.ms.fits
```

Press "`?`" to get all cursor commands of *splot* displayed. Leave the plot with "`q`". Images can be stacked with *scombine*.

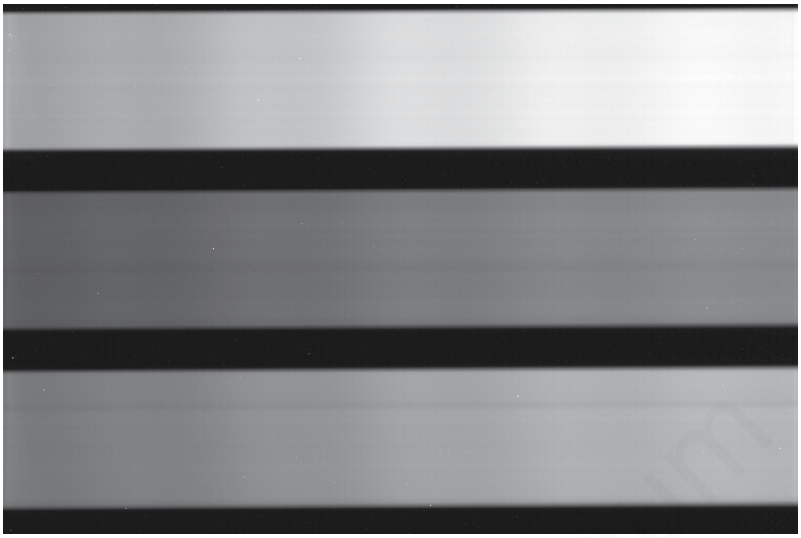

Figure B.10: A two dimensional not yet reduced flat field image. Taken with the 900-line grating and an exposure time of 600 s. The three slits can be seen. The illumination of the slits is different because of the different slit sizes. The periodic change of the amplitude is also visible with a period that is the same for all three slits. The period changes with the thickness of the glass plate that protects the CCD chip (`http://www.astrosurf.com/aras/fringing/schlatter/ripple.htm`, accessed on August 29., 2011).

B.5 Flats

Like other spectrographs the spectra taken with the DADOS spectrograph show spectroscopic fringes. These are presumably due to intereference effects on the glass plate protecting the CCD chip.[2] Figure B.10 shows a flat field image and Fig. B.11 the corresponding extracted spectrum. In both images the periodic change of the amplitude can be seen. To remove these fringes from the object frames it is necessary to divide the object frame by a flat field image, but this can not be done pixel by pixel as in photometry. The problem is that the pattern is not related to spacial coordinates (e.g. pixels), but to wavelength. It is necessary to extract and wavelength calibrate the flat field exposure and then divide the object frame by it according to their wavelengths (use the `sarith` task in IRAF). It is not necessary to take an image frame and flat field frame in the same night as long as the wavelength calibration is well done.
The flats have to be extracted and dispersion corrected exactly the same way as the object frames. When using *apall* it has to be paid attention that the spectrum of the flat is much broader than the one of a star because the whole slit is illuminated and so the apertures must be adapted. To divide a dispersion corrected object frame by a

[2] See `http://www.astrosurf.com/aras/fringing/schlatter/ripple.htm`, accessed on August 29., 2011.

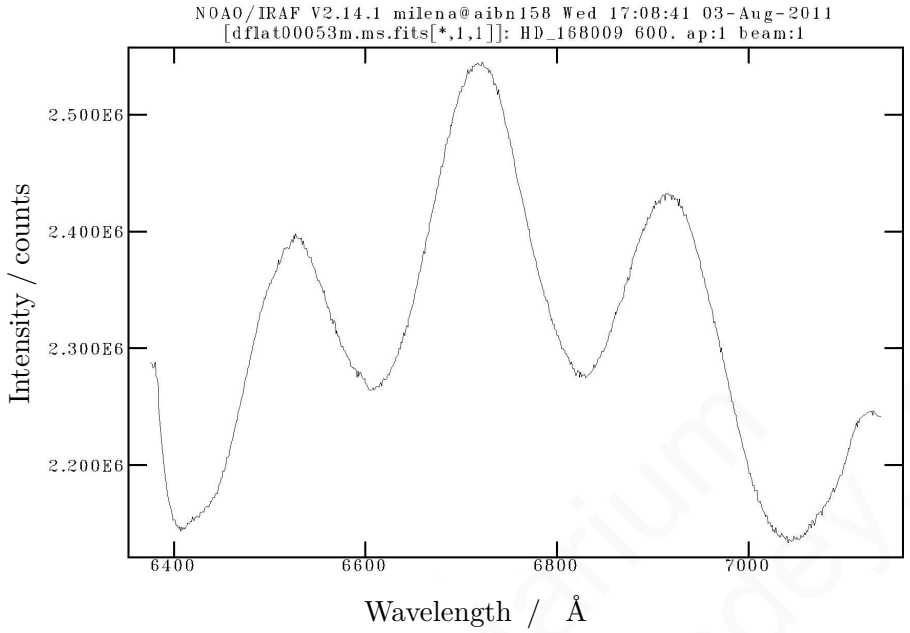

Figure B.11: Here is shown the flat field from Fig. B.10 but already extracted and wavelength calibrated. The periodic change of the amplitude is still visible.

dispersion corrected flat field, use the task *sarith*. If it does not work set the parameter `ignorea` at `epar sarith` to `yes`. Furthermore the wavelength range in `epar sarith` has to be set to the biggest range still included in both frames. Figure B.12 shows a spectrum of 44 Boötis that is not yet divided by a flat field in contrast to Fig. B.13 which shows the same spectrum but this time divided by a flat field.

B.6 Continuum Normalization

To normalize the spectra to the continuum, use the task *continuum*. Start the task, type in input and output image name whereupon the output image name should be indicated with a "`k`" in front of the name. So finally a dark subtracted, extracted, flattened and wavelength calibrated spectrum should be called `kdobj00255m.ms.fits`. If two spectra are supposed to be compared, pay attention to use the same fit function for the continuum fit. A "good" function is "spline3" with order 10.
The continuum fit for Wolf-Rayet stars is a little more tricky. If "spline3" with order 10 is used then IRAF identifies the big emission lines as continuum and erases them. Use a linear fit for Wolf-Rayet stars (function chebychev, order 1). Compare your spectrum to one from the literature (e.g. Fig. B.14) to see what is continuum and what is signal. With the cursor command "`s`" ranges can be selected where the continuum lies and IRAF will fit the linear function to the height of this continuum. Function and order can be

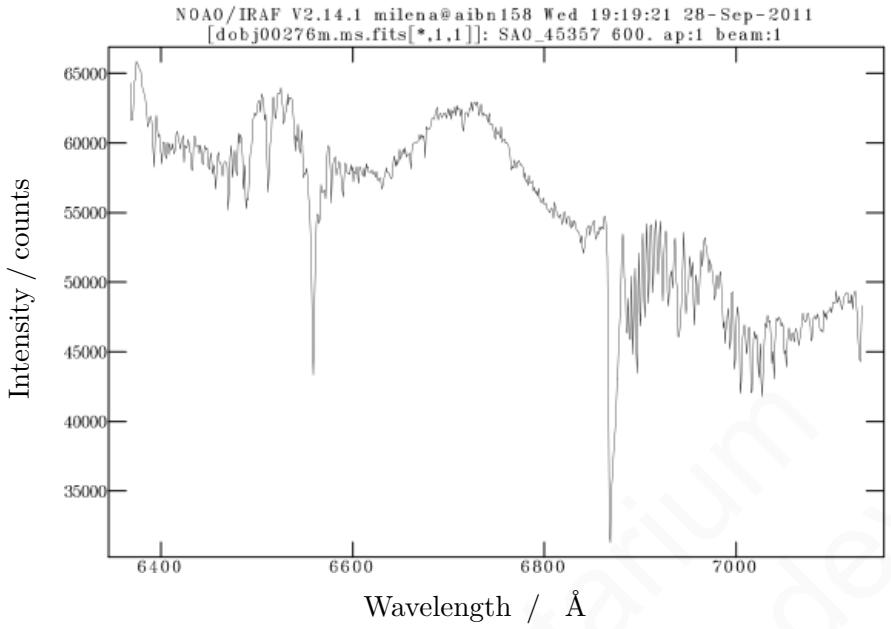

Figure B.12: Spectrum of 44 Boötis that is not yet divided by a flat field.

changed in `epar continuum`.

B.7 In short

- Generate a masterdark (`imcombine`)
- Subtract dark (`imarith`)
- Extract spectrum (`apall`)
- Extract spectrum of calibration lamp
  (`apall laser00004 out=claser00004 ref=obj00001m recen- trace- back- intera-`)
- Identify spectrum of calibration lamp (`identify`)
- Update header (`hedit obj00001m.ms.fits REFSPEC1 "claser00004.fits" add+ ver- show+`)
- Accomplish dispersion correction (`dispcor`)
- Divide by flat field (`sarith`)

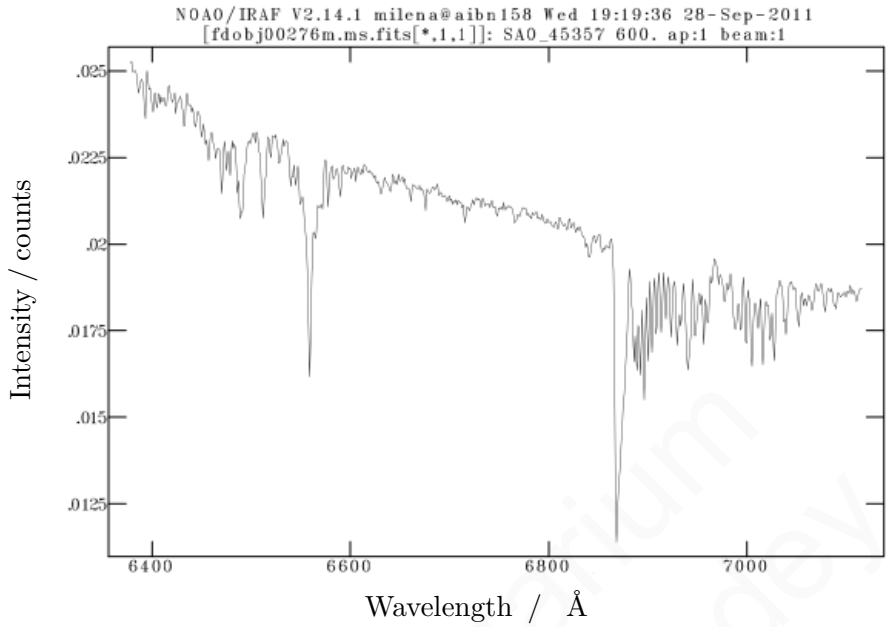

Figure B.13: Here is shown the same spectrum of 44 Boötis as in Fig. B.12 but this time divided by a flat field.

- Normalize to the continuum (`continuum`)

B.8 Analysis of spectral lines

We are interested in the widths of the spectral lines. These can be determined with the *splot* task. Start *splot* and activate the irafterm window. Press "`?`" for a list of cursor commands. It is possible to fit a Gaussian, Lorentzian or Voigt profile to the lines, depending if you press "`k`" and "`g`", "`k`" and "`l`" or "`k`" and "`v`". By fitting some lines just for fun you will notice that the displayed full-width-half-maximum depends on the start and ending points of the fit (the "`k`" and "`g`", "`l`", "`v`" position). To be able to compare the full-width-half-maxima of two images (e.g. maximum and minimum position of a binary system) it is important to do the fit between the same positions in the different images! Y-values have to lie in the continuum and x-values have to go, for example, 100 Å to the left and 100 Å to the right from the line. The choice of the x-coordinates is optional but needs to be consistent within the different images.
IRAF writes the fit parameters in the `logfile.cl`.

The images with the fitted spectral lines including the fit can be exported as .eps files. To get the .eps file type the following into the irafterm window (not IRAF terminal) which has to be activated.

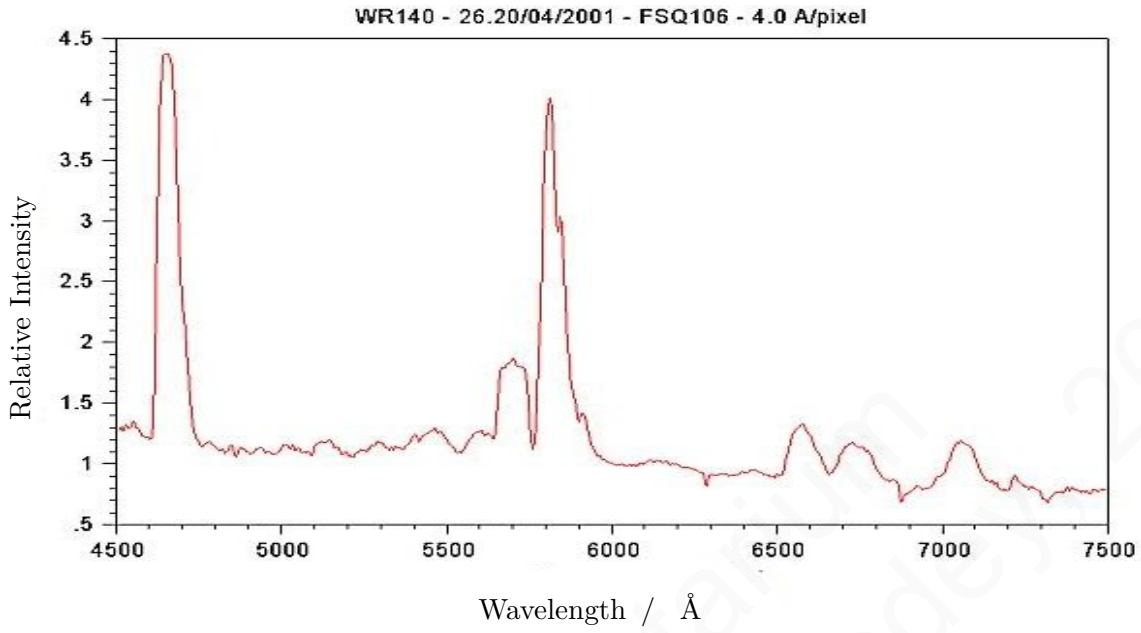

Figure B.14: Spectrum of WR 140 from `http://www.astrosurf.com/~buil/us/peculiar2/wolf.htm`, accessed on August 29., 2011.

- `:.snap eps`
- `:.gflush`

B.9 Signal-to-noise ratio

To determine the signal-to-noise ratio, the task *imexam* is used. Open the desired spectrum with `display imagename` in the SAO DS9 window, then start *imexam* in the IRAF terminal. Reactivate the DS9 window and press "`?`", IRAF now displays the possible cursor commands. "`m`" is for `statistics`. Under `epar imexam` the number of pixels (number of rows and columns) which are used for the statistics can be adjusted. Set it to 1 line and 20 columns (number of pixel = 20). Go back to the DS9 window and check the spectrum for ranges where there are no spectral lines. Put the cursor centered over the spectrum and press "`m`". The values are displayed in the IRAF terminal.

star name	magnitude of star	$T_{\mathbf{exp}}$/ s	S/N ratio
Vega	0.03	5	20
		15	22
		30	39
		60	37
		120	43
Regulus	1.36	10	13
		30	29
		60	32
SAO 61391	3.92	5	7
		10	7
		30	9
		60	16
		120	17
		300	39
AO Cassiopeiae	6.102	1200	28

Table B.1: Signal-to-noise ratios determined with the IRAF task *imexam*. The individual signal-to-noise ratio was determined in a narrow region in the continuum of the stellar spectrum in the original, two dimensional image before extraction of the spectrum. Note, that the signal-to-noise ratio depends also on the focus of telescope and spectrograph and on the weather (seeing). For example, it is shown here that after an exposure time of twenty minutes, the signal-to-noise ratio of AO Cassiopeia is still lower than 35. AO Cassiopeia rose late in that night and dawn already started. Nevertheless it is possible to obtain useful data of AO Cassiopeia with exposure times of 600 s. The magnitudes of the stars were taken from `http://simbad.u-strasbg.fr/simbad/`, accessed on August 29., 2011. It is shown how long the exposure time T_{exp} needs to be to obtain a desired signal-to-noise ratio depending on the magnitude of the star.

Appendix C

Spectra of Calibration Lamp

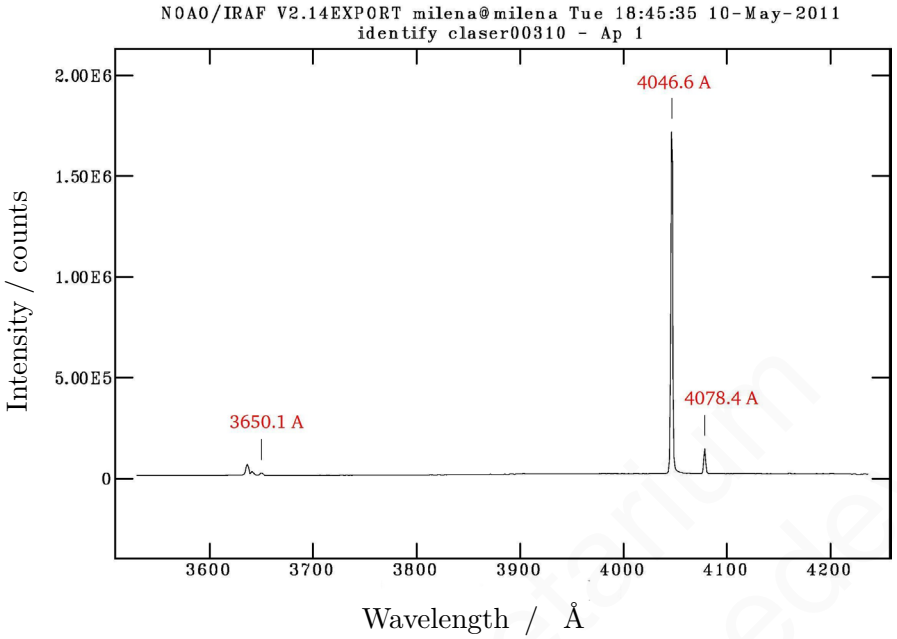

Figure C.1: Spectrum of calibration lamp for line identification.

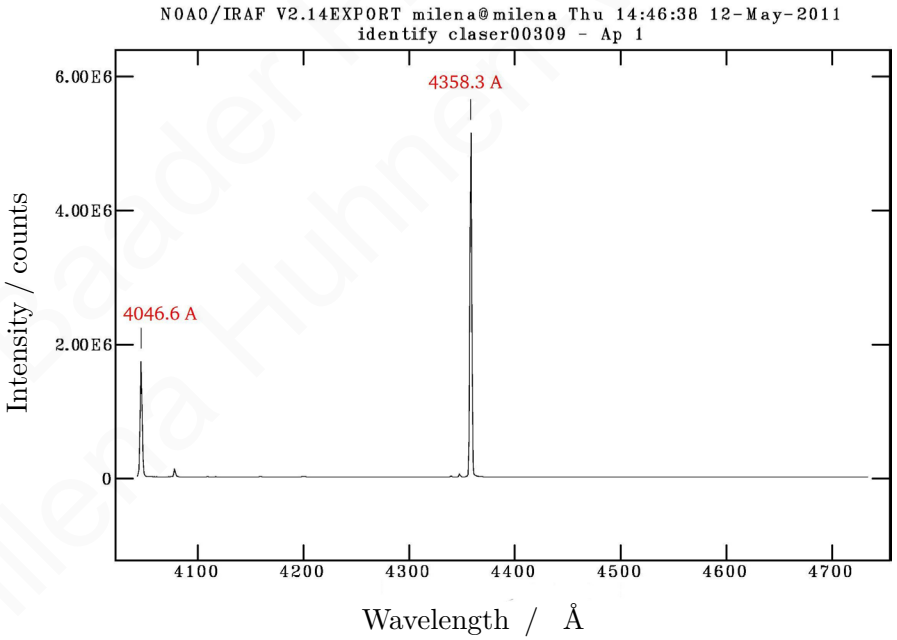

Figure C.2: Spectrum of calibration lamp for line identification.

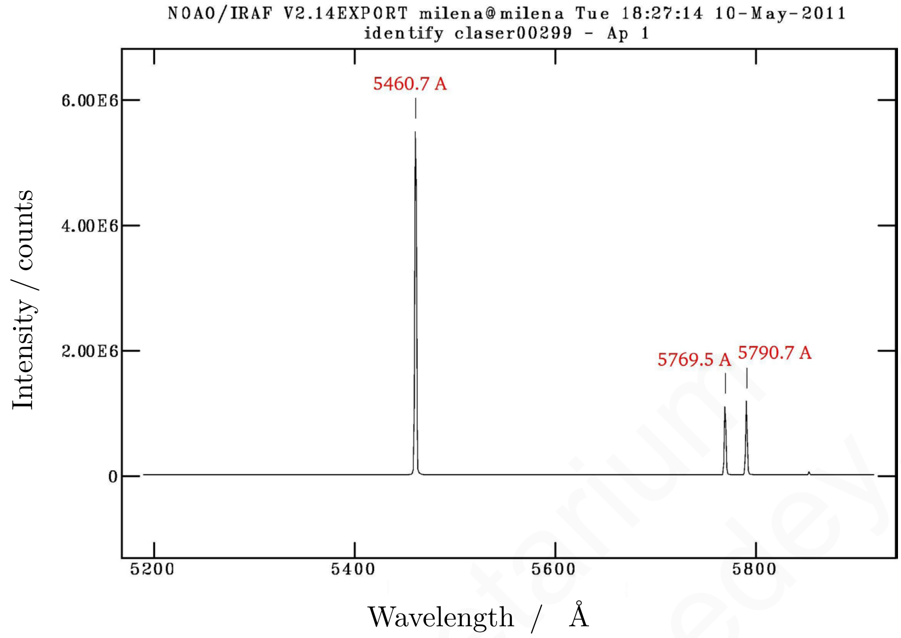

Figure C.3: Spectrum of calibration lamp for line identification.

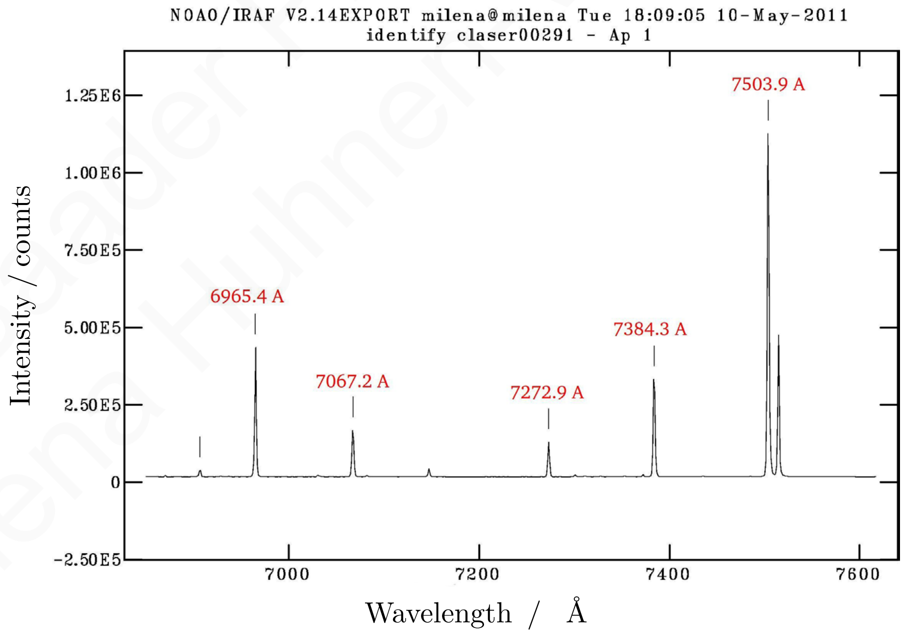

Figure C.4: Spectrum of calibration lamp for line identification.

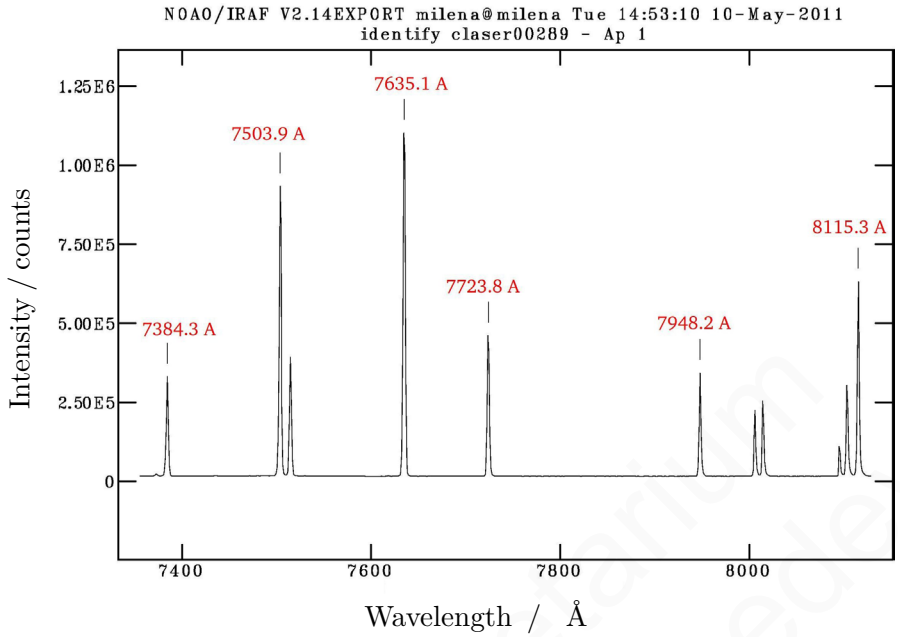

Figure C.5: Spectrum of calibration lamp for line identification.

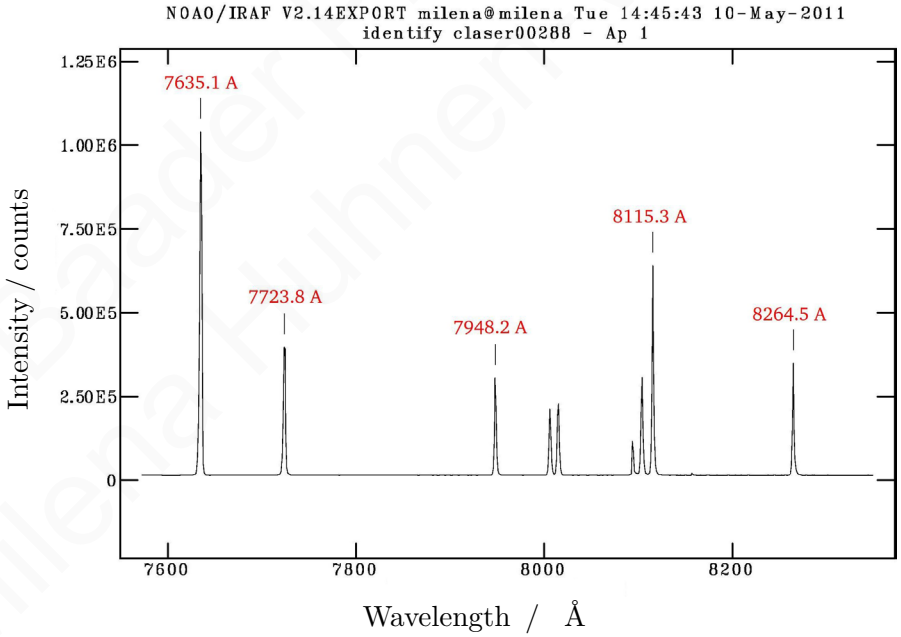

Figure C.6: Spectrum of calibration lamp for line identification.

Appendix D

Parameters of the SBIG ST 402 ME

CCD	
CCD	Kodak KAF-0402ME
Pixel Array	765 x 510 pixels
CCD Size	6.9 x 4.3 mm
Total Pixels	390,000
Pixel Size	9 x 9 microns
Full Well Capacity	~100,000 e-
Dark Current	1e¯/pixel/sec at 0° C
Antiblooming	Optional

Readout Specifications	
Shutter	Electromechanical
Exposure	0.09 to 3600 seconds, 10ms resolution
Correlated Double Sampling	Yes
A/D Converter	16 bits
A/D Gain	1.5e- unbinned 2.0e- binned 2x2, 3x3 (1.0e- and 1.4e- for ABG CCD)
Read Noise	13.8e¯ RMS Typical
Binning Modes	1 x 1, 2 x 2, 3 x 3
Pixel Digitization Rate	Up to 800,000 pixels per second with USB 2.0
Full Frame Download	<1 second

System Specifications	
Cooling - Enhanced	Single Stage Thermoelectric, Active Fan, -30 C from Ambient Typical
Cooling - Standard	Single Stage Thermoelectric, Active Fan, -20 C from Ambient Typical
Temperature Regulation	±0.1°C
Power	12VDC Power supply included
Computer Interface	USB 2.0 (USB 1.1 compatible)
Computer Compatibility	Windows 98/2000/Me/XP Mac OS-X

Physical Dimensions	
Optical Head	5 x 4 x 2.5 inches (including fan)
CPU	All electronics integrated into Optical Head, No CPU
Mounting	T-Thread, 1.25" nosepieces included
Weight	Approx. 20 oz. (0.6kg)
Backfocus (C-mount compatible)	0.69 inches

Figure D.1: Parameters of SBIG ST 402 ME given by the manufacturer. From `http://www.sbig.com/ST-402ME-C1.html` accessed on September 13., 2011.

Appendix E

Explanation of "Spectroscopic binary catalog"

Eighth Catalogue of the Orbital Elements of Spectroscopic Binary Systems

Alan H. Batten, J. Murray Fletcher, & D. G. MacCarthy
Dominion Astrophysical Observatory, Victoria, British Columbia, Canada

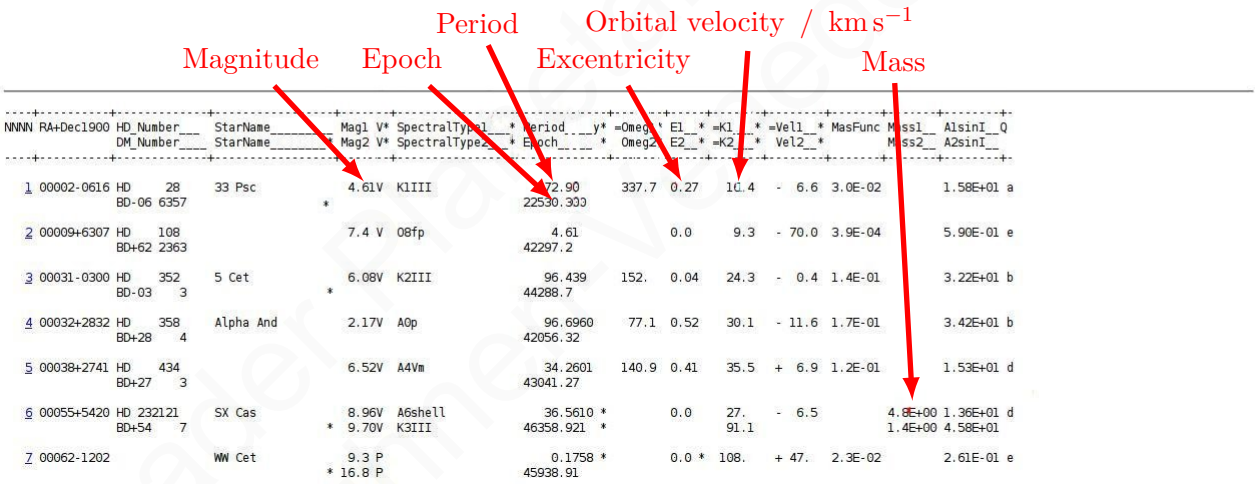

NNNN	RA+Dec1900	HD_Number / DM_Number	StarName	Mag1 V* SpectralType1	Mag2 V* SpectralType2	Period / Epoch	=Omega1 / Omega2	E1 / E2	=K1 / =K2	=Vel1 / Vel2	MasFunc	Mass1 / Mass2	AlsinI / A2sinI	Q
1	00002-0616	HD 28 BD-06 6357	33 Psc	4.61V K1III	*	172.90 22530.300	337.7	0.27	10.4	- 6.6	3.0E-02		1.58E+01	a
2	00009+6307	HD 108 BD+62 2363		7.4 V O8fp		4.61 42297.2		0.0	9.3	- 70.0	3.9E-04		5.90E-01	e
3	00031-0300	HD 352 BD-03 3	5 Cet	6.08V K2III	*	96.439 44288.7	152.	0.04	24.3	- 0.4	1.4E-01		3.22E+01	b
4	00032+2832	HD 358 BD+28 4	Alpha And	2.17V A0p		96.6960 42056.32	77.1	0.52	30.1	- 11.6	1.7E-01		3.42E+01	b
5	00038+2741	HD 434 BD+27 3		6.52V A4Vm		34.2601 43041.27	140.9	0.41	35.5	+ 6.9	1.2E-01		1.53E+01	d
6	00055+5420	HD 232121 BD+54 7	SX Cas	8.96V A6shell * 9.70V K3III	*	36.5610 * 46358.921 *		0.0	27. 91.1	- 6.5		4.8E+00 1.4E+00	1.36E+01 4.58E+01	d
7	00062-1202		WW Cet	9.3 P * 16.8 P		0.1758 * 45938.91		0.0 *	108.	+ 47.	2.3E-02		2.61E-01	e

Figure E.1: The spectroscopic binary catalog gives a detailed list of many binary star systems. To calculate the times when to observe the desired binary system, the epoch and the period are needed. For more accuracy it is advisable to look for more accurate values on the internet. The calculated mass can be compared to the mass given in the catalog. The listed orbital velocities must be added for the total orbital velocity. In some works about radial velocity curves, the amplitude of the curve is labeled with K, that's why in the catalog the orbital velocities are marked as K_1 and K_2.

Bibliography

Batten, A. H., Fletcher, J. M., & MacCarthy, D. G. 1989, Publications of the Dominion Astrophysical Observatory Victoria, 17, 1

Butler, K. & Giddings, J. R. 1985, Newsletter of Analysis of Astronomical Spectra, No. 9 (Univ. London), 9

Daflon, S., Cunha, K., de Araújo, F. X., Wolff, S., & Przybilla, N. 2007, AJ, 134, 1570

de Boer, K. S. & Seggewiss, W. 2008, Stars ans Stellar Evolution, ed. de Boer, K. S.

Giddings, J. R. 1981, PhD thesis, , University of London, (1981)

Howell, S. B. 2006, Handbook of CCD astronomy, ed. Howell, S. B.

Kippenhahn, R. & Weigert, A. 1990, Stellar Structure and Evolution, ed. Kippenhahn, R. & Weigert, A.

Kitchin, C. R. 1995, Optical astronomical spectroscopy, ed. Kitchin, C. R.

Kurucz, R. 1993, ATLAS9 Stellar Atmosphere Programs and 2 km/s grid. Kurucz CD-ROM No. 13. Cambridge, Mass.: Smithsonian Astrophysical Observatory, 1993., 13

Marchenko, S. V., Moffat, A. F. J., Ballereau, D., et al. 2003, ApJ, 596, 1295

Slettebak, A., Collins, II, G. W., Parkinson, T. D., Boyce, P. B., & White, N. M. 1975, ApJS, 29, 137

Acknowledgments

First of all I want to thank my thesis advisors **Norbert Langer** and **Robert Izzard** for their supervision.

Special thanks go to **Klaus Reif** for his encouragement and patience. Thank you that I could always come to you and knew I would find help and answers.

Thanks to **Dennis Proft**, **Verena Darmstädter**, **Jens-Peter Thiry**, **Thomas Perlitius** and **Jens Niederhausen** without whom I would not have had accomplished my studies.

The technical support from **Martin Polder**, **Philipp Müller** and **Henning Poschmann** was great. Without you I would not have been able to observe anything!

Ylva - Queen of IRAF - THANK YOU!!

I would like to show my gratitude to **Klaas S. de Boer** for his help concerning Wolf-Rayet stars and his tips how to improve my work.

When I started my thesis I was a total observer rookie and pretty lost in my first nights of observations. Thanks to **Alex Tudorica** and **Dominik Klaes**, who taught me everything and were always patient, I finally can call myself a real astronomer ;)

I would also like to thank **Andrea Stolte** for her encouragement, to always jolly me up when I lost the energy to keep working.

Speaking of support: I wish to thank **Aaron Ludlow**, **Ole Marggraf**, **Gisela Maintz**, **Ingo Thies**, **Michael Brockamp**, **Daniela Wuttke**, **Philipp Wilking**, **Lucia Klarmann**, **Nadya Ben Bekhti**, **Benjamin Winkel** and my **3.013 room mates**. And everybody else I forgot to mention...

Special thanks go to my **Mom** and my **Family**, **Hans und Hanna** and **Mirko** for accepting my stressful life and their efforts to keep as much stress away from me as possible. Danke!